DESIGN AND OPTIMIZATION OF A MIXED FLOW COMPRESSOR IMPELLER USING ROBUST DESIGN METHODS

A THESIS SUBMITTED TO
THE GRADUATE SCHOOL OF NATURAL AND APPLIED SCIENCES
OF
MIDDLE EAST TECHNICAL UNIVERSITY

BY

MERT ÇEVİK

IN PARTIAL FULFILLMENT OF THE REQUIREMENTS
FOR
THE DEGREE OF MASTER OF SCIENCE
IN
AEROSPACE ENGINEERING

SEPTEMBER 2009

Approval of the thesis:

DESIGN AND OPTIMIZATION OF A MIXED FLOW COMPRESSOR IMPELLER USING ROBUST DESIGN METHODS

submitted by **MERT ÇEVİK** in partial fulfillment of the requirements for the degree of **Master of Science in Aerospace Engineering Department, Middle East Technical University** by,

Prof. Dr. Canan ÖZGEN   _____
Dean, Graduate School of **Natural and Applied Sciences**

Prof. Dr. İsmail Hakkı TUNCER   _____
Head of Department, **Aerospace Engineering**

Asst. Prof. Dr. Oğuz UZOL   _____
Supervisor, **Aerospace Engineering Dept., METU**

Prof. Dr. İbrahim Sinan AKMANDOR   _____
Co-Supervisor, **Aerospace Engineering Dept., METU**

Examining Committee Members:

Prof. Dr. İbrahim Sinan AKMANDOR   _____
Aerospace Engineering Dept., METU

Asst. Prof. Dr. Oğuz UZOL   _____
Aerospace Engineering Dept., METU

Asst. Prof. Dr. İlkay YAVRUCUK   _____
Aerospace Engineering Dept., METU

Assoc. Prof. Dr. Sinan EYİ   _____
Aerospace Engineering Dept., METU

Asst. Prof. Dr. Sıtkı USLU   _____
Mechanical Engineering Dept., TOBB University

Date:_____09.09.2009___

I hereby declare that all information in this document has been obtained and presented in accordance with academic rules and ethical conduct. I also declare that, as required by these rules and conduct, I have fully cited and referenced all material and results that are not original to this work.

Name, Last name   : Mert ÇEVİK

Signature   :

ABSTRACT

DESIGN AND OPTIMIZATION OF A MIXED FLOW COMPRESSOR
IMPELLER USING ROBUST DESIGN METHODS

ÇEVİK, Mert

M.Sc., Department of Aerospace Engineering

Supervisor: Assoc. Prof. Dr. Oğuz UZOL

Co-Supervisor: Prof. Dr. İbrahim Sinan AKMANDOR

September 2009, 100 pages

This is a study that is focused on developing an individual design methodology for a centrifugal impeller and generating a mixed flow impeller for a small turbojet engine by using this methodology. The structure of the methodology is based on the design, modeling and the optimization processes, which are operated sequentially. The design process consists of engine design and compressor design codes operated together with a commercial design code. Design of Experiment methods and an in-house Neural Network code is used for the modeling phase. The optimization is based on an in-house code which is generated based on multidirectional search algorithm. The optimization problem is constructed by using the in-house parametric design codes of the engine and the compressor. The goal of the optimization problem is to reach an optimum design which gives the best possible combination of the thrust and the fuel consumption for a small turbojet engine.

The final combination of the design parameters obtained from the optimization study are used in order to generate the final design with the commercial design code. On the last part of the thesis a comparison of the final design and a standard radial flow impeller is made in order to clarify the benefit of the study. The results have been showed that a mixed flow compressor design is superior to a standard radial flow compressor in a small turbojet application.

Key-words: Mixed flow compressor, turbojet engine, design methodology, optimization, Multi Directional Search Algorithm, Design of Experiments, Neural Networks

ÖZ

KARIŞIK AKIŞLI BİR KOMPRESÖRÜN ROBUST TASARIM METODLARI
KULLANILARAK TASARIM VE OPTİMİZASYONU

ÇEVİK, Mert

Yüksek Lisans, Havacılık ve Uzay Mühendisliği Bölümü

Tez Yöneticisi: Yrd. Doç. Dr. Oğuz UZOL

Ortak Tez Yöneticisi: Prof. Dr. İbrahim Sinan AKMANDOR

Eylül 2009, 100 sayfa

Bu çalışma, santrifuj bir impeller'ın geliştirilmesi için kullanılacak bir tasarım metodolojisinin geliştirilmesini ve bu metodolojinin kullanılarak küçük turbojet motorları için karışık akışlı bir impeller'ın tasarımını kapsamaktadır. Metodoloji birbiri ile etkileşim halinde çalışan, tasarım, modelleme ve optimizasyon süreçlerini bünyesinde barındırmaktadır. Tasarım süreci, birbiri ile uyumlu olarak çalışan bir dizi kod ve ticari tasarım yazılıınmdan oluşmaktadır. Modelleme prosedürü, Deney Tasarımı Yöntemine dayanılarak kurulan bir veri tabanının bir Yapay Sinir Ağı koduna bağlı olarak sürülmesi ile oluşturulmuştur. Optimizasyon işlemi, Çok Yönlü Arama Algoritması üzerine çalışan bir optimizasyon kodu tarafından gerçekleştirilmektedir. Optimizasyon problemi, çalışma bünyesinde hazırlanan parametrik kompresör ve motor tasarım kodları ile hazırlanmıştır. Optimizasyon probleminin hedefi, verilen şartlar dahilinde küçük bi turbojet motoru için olabilecek en iyi itki-yakıt sarfiyatı kombinasyonunu veren tasarım parametrelerine ulaşmaktır.

Optimizasyon sonucunda elde edilen tasarım parametreleri kombinasyonu kullanılarak ticari bir yazılım vasıtasıyla nihai tasarım oluşturulmaktadır. Çalışmanın son bölümünde, ortaya çıkan tasarım yapılan çalışmadan elde edilen faydayı gösterebilmek amacıyl standart bir radyal kompresör ile karşılaştırılmaktadır. Sonuçlar, küçük turbojet uygulaması için, karışık akışlı bir kompresörün radyal akışlı bir kompresörden çok daha avantajlı olduğunu göstermiştir.

Anahtar Kelimeler: Karışık akışlı kompresör, turbojet motoru, tasarım metodolojisi, optimizasyon, çok yönlü arama algoritması, deney tasarımı, yapay sinir ağı

ACKNOWLEDGEMENTS

I am grateful to my supervisor Asst. Prof. Dr. Oğuz UZOL for his professional support, guidance, friendship and encouragement throughout the completion of this thesis work. I deeply appreciate his patience and many efforts to proofread my thesis and papers over and over again.I would
like to thank to Prof. Dr. Sinan Akmandor who inoculate me the enthusiasm of propulsion and his limited but very effective supervising during this study.

Thanks to Dr. İlkay Yavrucuk for his great support about, constructing the optimization part of this study and allowing me to use the Neural Networks code written by him.

Special thanks to Dr. Atılgan Toker, whom shows me a tolerance about finishing this study, instead of workload in Roketsan.

I would like to express my sincere appreciation to God, who makes me able to enjoy from, good wine, fine cheese, well flavoured coffee and esthetics that makes me able to live during my poor life.

TABLE OF CONTENTS

LIST OF TABLES

LIST OF FIGURES

FIGURES

xiii

xiv

LIST OF SYMBOLS

a	Speed of Sound [m/s]
b	Impeller blade height [mm]
c	Absolute Velocity [m/s]
D	Impeller diameter [mm]
DR	Impeller diffusion ratio
e_c	Polytropic Efficiency of the compressor
e_t	Polytropic Efficiency of the turbine
$F_{specific}$	Specific Thrust [Ns/kg]
f	Fuel to air ratio
h_{PR}	Internal energy of the fuel
I	Incidence [°]
M	Mach Number
$\dot{m}$	Mass Flow Rate [kg/s]
N_b	Main Blade Number
OR	Operating Range
t	Thickness [mm]
U	Tangential Velocity [m/s]
w	Relative Velocity [m/s]
W	Work
α	Absolute gas angle with respect to radial direction [°]
β	Blade Angle [°]
δ_{2p}	Deviation at impeller exit
ζ	Compressor inlet hub to tip ratio
η	Component Isentropic Efficiency
η_{th}	Thermal efficiency

η_p	Propulsive efficiency
η_o	Overall efficiency
η_m	Mechanical efficiency
η_a	Effectiveness of element a in two-zone model
η_b	Effectiveness of element b in two-zone model
π	Component Total pressure ratio
σ_f	Slip Factor
τ_λ	Technology Parameter
τ	Component Total temperature ratio
φ	Meridional Angle [°]
χ	Ratio of mass flow rate in secondary region to primary region
ϕ	Flow Parameter
ω	Rotational speed [rpm]

Subscripts:

b	Burner
c	Compressor
f	Fuel
h	Hub
r	Radial Component
o	Air
t	Turbine
t	Tip
z	Axial Component
1	Impeller inlet
2	Impeller exit
θ	Tangential Component

CHAPTER 1

INTRODUCTION

Unmanned Air Vehicles (UAV's) have become a rising trend in military operations since the beginning of the 1990's. There are numerous studies on UAV development for a broad range of applications. As survivability and effectiveness are indispensable requirements for UAV's, high performance becomes a vital need. However, size and weight limitations, cause great contradictions with survivability the performance needs of UAV's [1]. These contradictions force designers to focus on propulsion system solutions that have high power density and small size, such as small gas turbine engines.

There have been few attempts that investigated small gas turbine integration to unmanned vehicles since 1980's. The main reason is that, the space and weight limitations cause low efficiency and lack of performance problems due to limited cross sectional area. Nevertheless there are promising solutions that are unconventional for normal size gas turbine engines. One of these solutions is, the utilization of mixed flow compressors which offer the capability of high mass flow rate and pressure ratio, in a single stage for an engine with limited cross sectional area.

Mixed flow compressor is a type of a centrifugal compressor that has a meridional exit angle between 0 and 90 degrees. This geometrical feature helps to combine the advantageous sides of axial and centrifugal compressors in mixed flow configuration. High pressure ratio in single stage, relatively high mass flow rate in a limited cross section area and broad

operation range with a robust flow regime [2] can be obtained in a mixed-flow design. These advantages are handicapped due to a weight increase which is the result of a longer impeller [2].

This weight increase can be unacceptable for an aero - gas turbine, which basically prevented the development of mixed-flow compressors for decades. However, this deficiency becomes less critical as the size of the engine gets smaller. In Figure 1.1 which is constructed using the data given in Monig et al [3], the distribution of compressor types used in small gas turbines until 1990's is presented according to their performance parameters. The compressor type of each engine in the figure, is marked as A:Axial, R:Radial, and M:Mixed. The numbers on the markers show the number of stages on the axial compressor. It can be seen from this chart that, in small aero gas turbine engines designed mixed flow configuration is rarely used until 90's, which is probably a result of unfamiliarity of designers to this type of a compressor. According to this data, the first attempt in this study was to understand the performance characteristic of a mixed flow compressor and to show the feasibility of this kind of a compressor on a small gas turbine engine.

The structure of the study is based on a design and optimization methodology, which organizes design procedures from different levels and reaches a final design after an optimization process. A noteworthy feature of this procedure is its robustness, which may be defined as the ability of the methodology to give a reasonable result to any input. The robustness of the methodology comes from the structure that verifies the results of the previous step in each new step. Also, the methods embedded to the methodology such as Neural Networks improves the numerical side of this ability with their numerical robustness. However, it should also be noticed that, the effectiveness and the reliability of this feature highly depends on the database that it relies on. For this reason, a special method called Design of

Experiments (DoE) is used for database generation in this study. A brief explanation of the background and application of this methodology will be given in upcoming parts of this thesis.
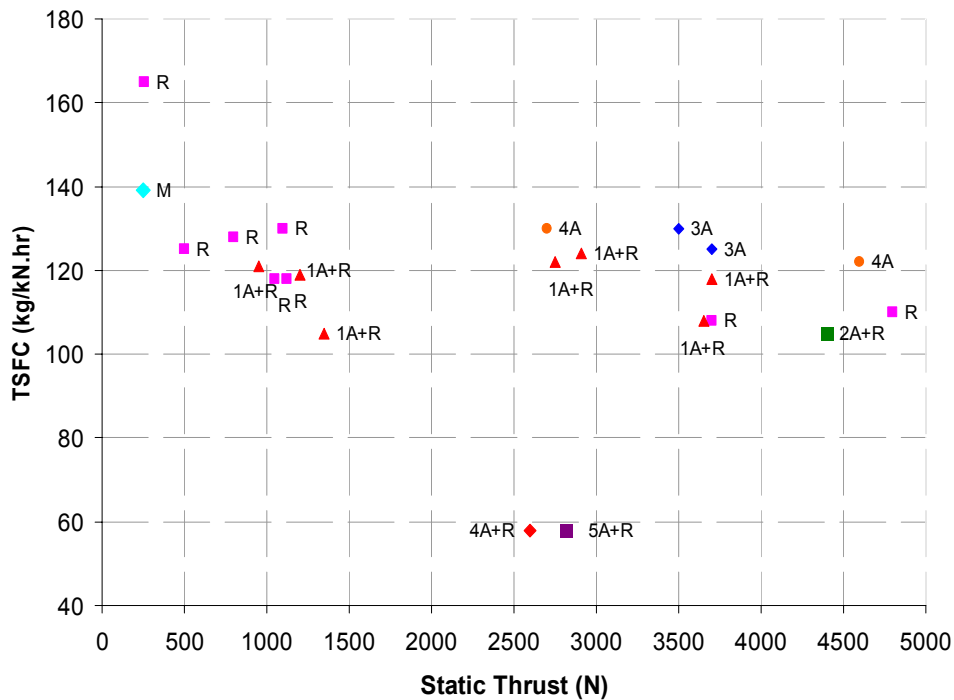
Figure 1.1 – Performance distribution of various small to medium sized turbojet engines [3].

1.1 Literature Survey

The studies about the mixed flow compressors cen be found in detailed reports published by NACA in 1950's. Goldstein [4] presented the design and experimental performance investigation of an axially discharged mixed flow compressor, adapted especially for jet engines. Similar studies continued in 1950's, including experimental work by Douglas et al. [5], and theoretical studies for flow analysis made by Harmick et al.[6] and Stanitz [7]. Although a significant amount of research have been done on mixed flow

compressors, the rising trend of the multistage axial compressors prevented the evolution of these devices after 1950's.

In 1980's, mixed flow compressors were revived by Monig et al [3] on the application of highly loaded mixed flow compressors to the small gas turbine engines. In this study, Monig compares compressor types for small gas turbine applications and presents a vision on the causality of using mixed flow compressors for small jet engines. Same kind of studies are also presented by Eisenlohr et al [2], and Musgrave et al [8] about the design of highly loaded mixed flow compressors. Further studies of Monig focused on the design of a mixed-flow supersonic compressor [9]. A more recent study using mixed-flow compressors is an expandable small turbojet application the TJ-50 engine presented by Harris et al [10].

Advanced understanding of the physics of turbomachinery flows in the past few decades, increased the accuracy of 2-D and Quasi 3-D solution methods. This resulted in the generation of design methods, which combine statistical tools and numerical optimization methods in a reliable design environment. One these efforts is presented by Pauer and Nrobert [11], which is a rapid design tool based on simple through flow solver and the results of the solver are coupled with a three-dimensional blade generating tool. A computation method presented by Stanitz and Prian [12] is used in order to generate the velocity distributions in blade to blade section. Although the reliability of the results are not presented clearly, the structure of the study is a good example of such a design methodology. A much more complicated but reliable design could be found in the study presented by Japikse and Pratt [13] which is basically, the design methodology based on a commercial design software called, Concepts NREC. This methodology is explained as an integrated tool that consists of a meanline design, sophisticated three-dimensional blading design and numerical methods coming from Computational Fluid Dynamics (CFD). Pelton [14] explains the

empirical models used in Compal which is the one dimensional design module of NREC. This study organizes a broad experimental data base to generate diffusion models implemented in the Compal.

A good source for understanding the setup of a turbomachinery optimiziation problem is the detailed design and optimization study presented by Benini [15]. This study briefly describes how to parametrize and build up an optimization problem for a compressor. It is also a valuable guide especially on determining the compressor design parameters considering their priority in the optimization process.

An important improvement to the design studies explained above can be obtained by adding numerical optimization to the process which is generally used coupled with statistical analysis tools. Using specialized tools such as Neural Network, Design of Experiments and numerical optimization methods like multidirectional search algorithm is such an effort. An example of this kind of a study is design optimization of a radial compressor using Design of Experiments and Radial Basis Neural Network together for a detailed design process, which is presented by Kim et al. [16]. Another study presented by Mouli et al.[17] is also such an effort that generalizes the coupled application of these two methods on a simple optimization algorithm.

Obtaining a reliable and robust design methodology that considers the design space under given conditions, and analyzes this space using numerical optimization methods in a well defined problem is a crucial need for today's industry. This kind of a design process is not typically combined under a single design methodology. This study attempts to formulate such a structure and demonstrates on the design optimization of a mixed flow compressor impeller.

1.2 Objectives

The objective of this study is to develop a design optimization methodology that could generate an optimum centrifugal compressor impeller design. The methodology covers the design process from the initial conceptual phases, to the end of the preliminary design phase. Design studies in the literature generally focus on the detailed design process which mostly involves CFD solutions and their validations. There is not sufficient information on how to design and optimize a compressor from beginning to the end of the design process. Therefore, this thesis concentrates on converting, relating and reflecting the basic performance requirements of a small gas turbine engine to the design of the compressor through a robust design optimization procedure.

The presentation of this thesis is structured on three main parts, the design methodology, sample design study and the detailed analysis of the final design.

The structure of the design methodology and the theory of each part of the methodology is given in Chapter 2. The theory for one-dimensional computation tools, the Design of Experiments methods, the theory of Neural Networks and related Leuvenberg-Marquardt algorithm and the theoretical background of direct search algorithm based optimization method is given in this chapter.

Chapter 3 presents the results of a sample design problem. The characteristics of mixed flow compressors, the explanation of small turbojet engine design problem and the structure of the optimization problem is mentioned. The final design generated from the results of optimization study is presented in this chapter.

Chapter 4 presents an analysis of the optimized design using CFD. Modifications made on the final design according to CFD results are also described in this chapter.

Chapter 5 includes summary and conclusions as well as the future work that can be done in order to improve the study.

The detailed geometry and performance data of final compressor design is given in Appendix A.

CHAPTER 2

DESIGN AND OPTIMIZATION METHODOLOGY

2.1 Design Algorithm

The design algorithm is constructed in such a way that it can handle the design process starting from the design requirements to the end of the detailed design. The algorithm consists of three main parts which are, design, modeling and optimization. These three parts are implemented into the algorithm using various commercial and/or in-house codes which are linked to each other with input-output relationships. The completion of these processes results in a final optimized geometry. The block diagram representation of the design optimization algorithm can be seen in Figure 2.1.

The design algorithm starts by setting the performance requirements of the engine. As the engine performance is set, the required compressor performance is obtained by using an engine parametric cycle design code. Afterwards, the reference geometry of the compressor is obtained using an in-house one dimensional compressor design code called ParaComp from the desired performance requirements. As a result, the reference values and constraints needed to build up the optimization problem is determined.

The modeling procedure consists of three steps. In each step a different method is used because each method has its own advantages. First, the optimization problem is defined, which involves determining the decision variables, constraints and the cost function. Therefore, a function is needed that relates the decision variables with the cost expression. This determines

the next two steps of the modeling procedure, which are the database generation and then obtaining the function by using Neural Networks.

The database generation is based on a experiment chart that is determined by using Design of Experiments. The samples in database are generated by using a turbomachinery design software called Concepts NREC, which gives a precise and rapid design capability in both one, two and quasi-three dimensional design space [13]. After the construction of the database, the compressor performance data is converted to the engine performance data by using the engine design code. At the end, a database is obtained, which relates the decision (optimization) variables to the cost function that consists of engine performance parameters. This database is used to train a Neural Network code and finally a function is obtained that can be used in the optimization procedure.

In the third part of the algorithm, the function obtained from Neural Network is optimized in order to minimize the cost function using an in-house optimization code. The optimum geometric parameters are obtained at the end of the process, which are five selected key design parameters that describe the compressor geometry. As the last part of the algorithm, a final design is obtained by using NREC according to the optimum decision parameters. Finally the performance of the final design is checked using the in-house cycle code and an aircraft performance code. Detailed descriptions of all procedures described above are given in the following sections.
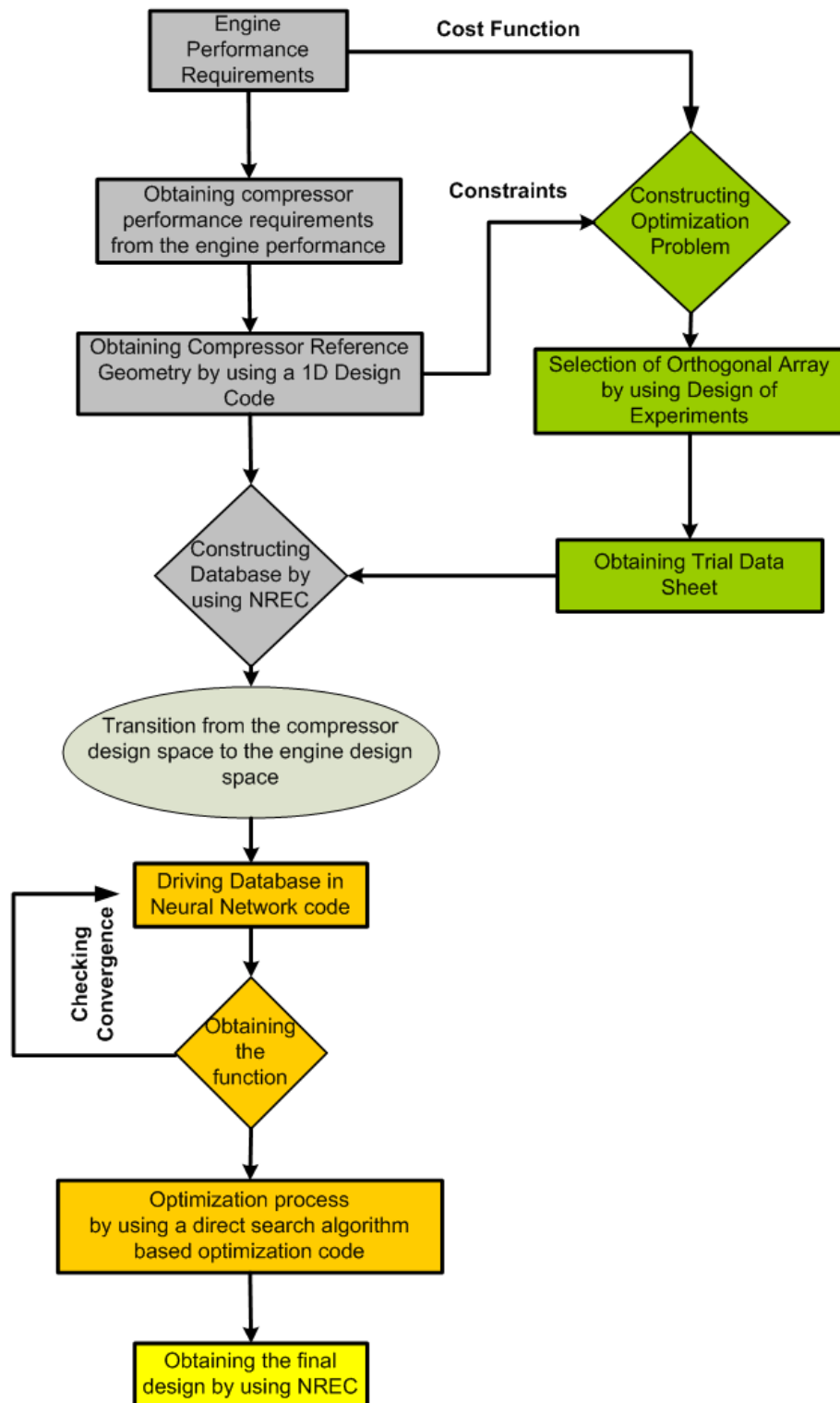
Figure 2.1 – Block diagram of the design algorithm

2.2 Parametric Cycle Code

Parametric cycle calculations are obtained using an in-house cycle code which is developed using the methodology given in Mattingly et al [18] for a turbojet engine.

The cycle calculations are based on the assumptions given below [18];

•   The flow is on the average steady

•   The flow is one-dimensional at the entry and the exit of each component and each axial station

•   The fluid behaves as a perfect gas

•   For the case of variable specific heats, the NASA Glenn thermochemical data and the Gordon-McBride equilibrium algorithm are used to obtain thermochemical properties of air and combustion gasses at any station.

The algorithm of the code is based on calculation of thermodynamic conditions of air or air-fuel mixture in each reference station shown in Figure 2.2.
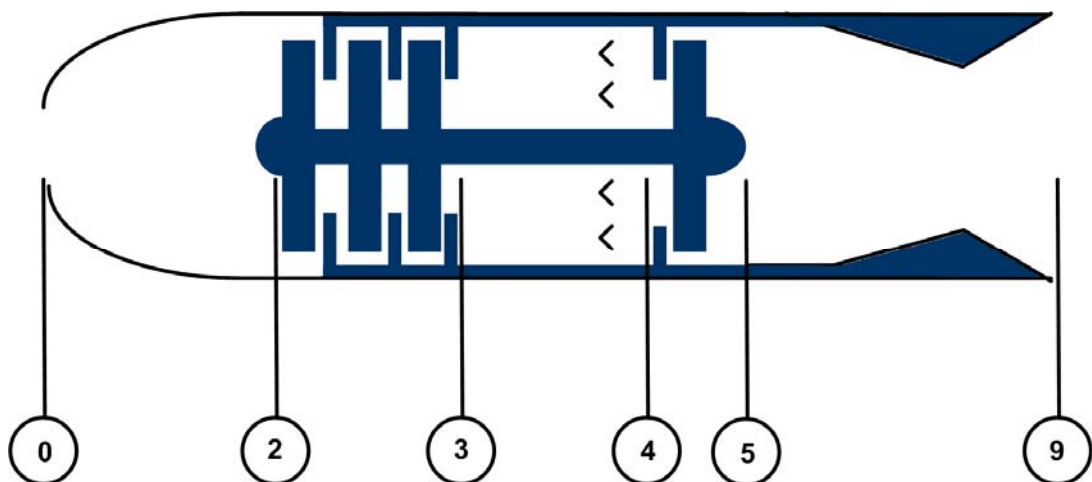
Figure 2.2 – Reference Stations for a Turbojet Engine

The input parameters are classified under three categories given below. The first one is the flight condition which comes from the mission profile of the air vehicle. The fuel heating value is a design limitation that comes from the characteristics of the fuel and it depends on the fuel selection of the designer. The parameters that are grouped under "component figure of merit", are the parameters which are assigned by using empirical formulas or typical data from the literature. These parameters determine success of simulation of the physical condition of the problem and accuracy of the results. In this study, as there is no available empirical formula, the data taken from the literature are assigned to the parameters. The results obtained with these values are validated again with the data obtained from the literature. Design choices are the parameters given by the designer, which have a direct effect on the performance characteristics of the engine. Input parameters of the code are listed in Table 2.1.

Table 2.1 Inputs of the Parametric Cycle Code

Inputs	
Flight Parameters	M_0, T_0, P_0
Fuel heating value	h_{PR}
Component figures of merit	π_b, π_{dmax}, π_n, η_b, η_m, e_c, e_t
Design Choices	π_c, T_{t4}, $F_{required}$

Outputs of the code are the parameters, that shows the performance behavior of the engine and the components. These parameters are given in Table 2.2

Table 2.2 Outputs of the Parametric Cycle Code

Outputs	
Overall performance	$\dot{m}_0$, f_0, S, $F_{specific}$, η_p, η_{th}, η_o
Component behavior	π_t, τ_c, τ_t, τ_λ, η_c, η_t, W_t, W_c, M_9, P_{t9}/P_9, P_9/P_0, T_9/T_0

The code, does not give a single result but it gives a set of results which shows different result combinations. These combinations are obtained by an iteration process based on changing π_c and T_{t4} values in an interval. By this way, the user has a chance to see and select the most suitable alternative in the generated results. Main formulas used in the cycle calculations are;

$$\eta_c = \frac{\pi_c^{\gamma-1/\gamma}-1}{\tau_c} \tag{2.2.1}$$

$$\tau_c = \pi_c^{\gamma-1/\gamma e_c} \tag{2.2.2}$$

$$f = \frac{\frac{C_{P3}\tau_r\tau_c\tau_d}{C_{P0}}-\tau_\lambda}{\tau_\lambda-\eta_b\frac{h_{PR}}{C_{P0}T_0}} \tag{2.2.3}$$

$$\tau_\lambda = \frac{C_{P4}T_{t4}}{C_{P0}T_0} \tag{2.2.4}$$

$$\pi_t = \tau_t^{\gamma-1/\gamma e_t} = 1 - \frac{\tau_r}{\eta_m(1+f)\tau_\lambda}(\tau_c - 1) \tag{2.2.5}$$

$$\eta_t = \frac{1-\tau_t}{1-\pi_t^{\gamma-1/\gamma}} \tag{2.2.6}$$

13

$$F_{specific} = F/\dot{m}_0 = a_0 \left[\frac{\dot{m}_9}{\dot{m}_0} \frac{V_9}{a_0} - M_0 + \frac{\dot{m}_9}{\dot{m}_0} \frac{R_9}{R_0} \frac{T_9/T_0}{V_9/a_0} \frac{\left(1 - P_0/P_9\right)}{\gamma} \right]$$

(2.2.7)

$$\eta_P = \frac{\left(F/\dot{m}_0\right)}{a_0 \left(\frac{1+f}{2}\left(\frac{V_9}{a_0}\right)^2 - \frac{M_0^2}{2}\right)}$$
(2.2.8)

$$\eta_{th} = 1 - \frac{C_{P0}/C_{P3}}{\tau_r \tau_c \tau_d}$$
(2.2.9)

$$\eta_O = \eta_p \times \eta_{th}$$
(2.2.10)

2.3   One Dimensional Compessor Design Code

Flow through the blade passages of a typical radial impeller may include both accelerating and diffusing regions and is subject to the effects of viscous shear, flow path curvature and Coriolis forces due to rotation. Several analytical models, of varying complexity and accuracy, have been developed to aid in the design process. The most basic type of design analysis used is a one dimensional (1-D) or station-by-station analysis, commonly referred to as meanline. 1-D analyses are based on a finite control volume analysis and yield predictions of the mass averaged output conditions without performing detailed modeling of the entire flow path. 1-D design calculations may become very effective tools, if they are supported by reliable empirical models, statistical calculation tools and advanced graphical interfaces.

An example of this kind of a 1-D design code is Compal, which is a commercial software used also in this study. However, if there is no idea

about dimensions and rotational speed at design point the design process may become complicated from the beginning of initial steps. So that it is much more easy and practical to start the design process by introducing a more basic code, instead of an advanced and relatively complicated program. Paracomp is a 1-D design code which is generated for such a purpose.

Paracomp is a one dimensional in-house design code, which is based on, energy equation, velocity correlations and empirical correlations about performance. The objective of the code is to build a relation between performance needs and the geometry in order to help the designer to make an initial sizing. The equations embedded to the code only computes the entrance and the exit of the compressor. Structure of the algorithm arranged in order to compute the impeller shape that accomplishes the desired change in flow. The code can be used for both purely radial and mixed flow compressors.

The calculations are based on the assumptions given below;

- The flow is on the average steady
- No inlet guide vane is used and no preswirl is given in the computations. So the flow is one-dimensional at the entry of the compressor.
- The fluid behaves as a perfect gas

The user-defined inputs of the code are, pressure ratio, mass flow rate, rotational speed, blade number, backsweep value (β_2) at the exit, meridional exit angle (φ_2) and isentropic efficiency. The first four inputs are regular parameters which are common in most of the commercial design codes. Only the efficiency is an unusual parameter which is mostly determined from empirical models. However in this study, as there is an unconventional

design case, none of the empirical models gave a realistic result. Consequently, it's decided to give some common efficiency values, taken from the literature, directly as an input to the code. In addition to these primary inputs, there are secondary inputs which are embedded to the code, like inlet flow characteristics. The final input type is design limitations, which is important to achieve appropriate outputs.

Outputs of the code are the geometry and the velocity triangles at inlet and exit of the impeller. Although these outputs do not give any sense about the flow phenomena in blade passages, it gives enough information to make a good prediction in order to start a design optimization study.

There are two iterative parameters in the algorithm, which are the inlet Mach Number and the mass flow parameter. The iterative procedure based on these parameters, prevents the algorithm to find an inappropriate geometry that can mislead the user in detailed design. This part of the algorithm is mostly based on experience and knowledge coming from literature and previous design studies. At the end of this procedure, a group of results are obtained which gives the same performance in different geometries. The code eliminates undesirable results according to the design limitations and gives a final output. The algorithm of the code is represented in Figure 2.3 as a block diagram.
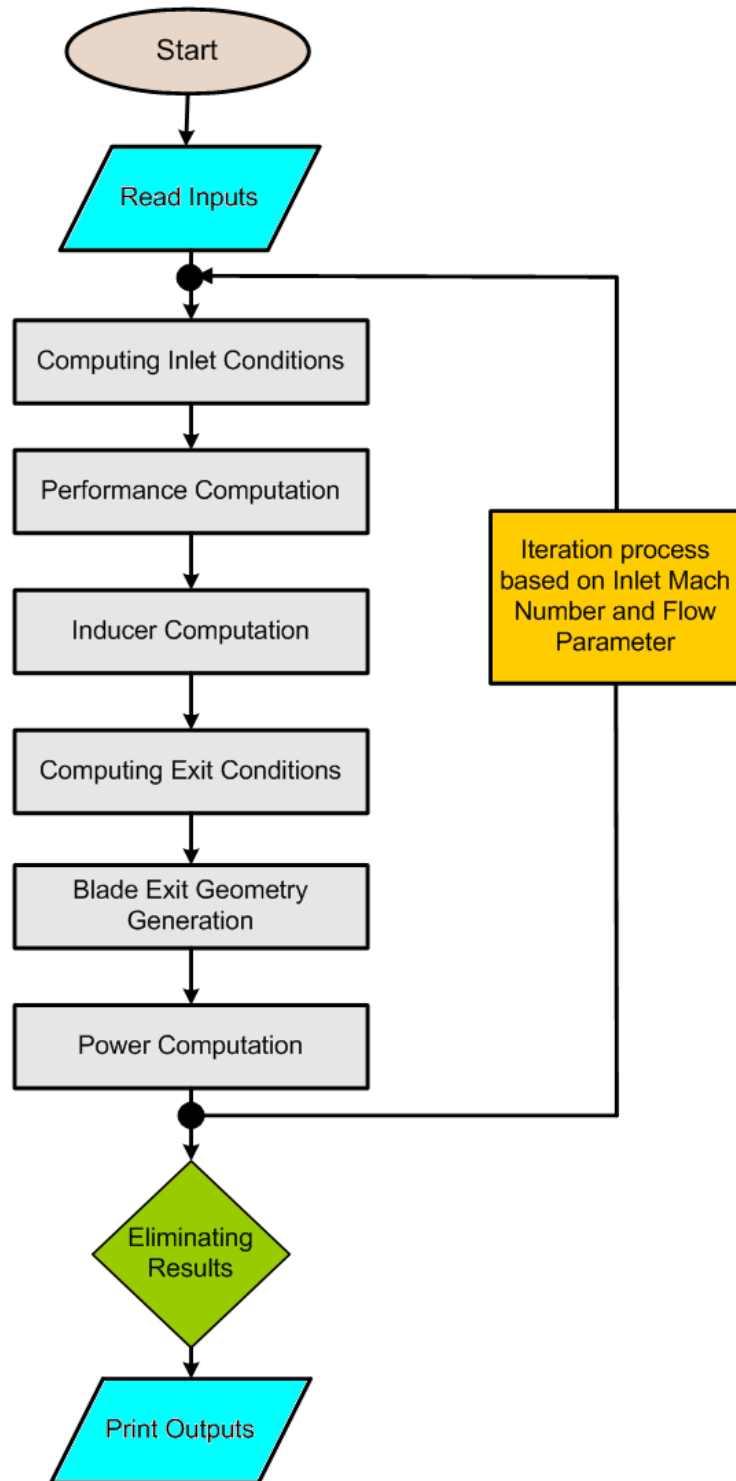
Figure 2.3 – Block diagram of the algorithm of Paracomp

Main formulas used in the cycle calculations are derived from the performance relations given in Hill and Peterson [19];

Exit Geometry and Performance;

$$\pi_C = \left[1 + \eta_C \left(\frac{U_2}{a_{01}}\right)^2 (\gamma - 1)\left(1 - \frac{w_{r2}}{U_2}\frac{\tan\beta_2}{\sin\varphi_2}\right)\right]^{\gamma/\gamma-1} \qquad (2.3.1)$$

$$U_2{}^2 = \frac{a_{01}^2\left(\pi_C{}^{\gamma-1/\gamma-1}\right)}{\eta_C(\gamma-1)\left(\left(1-\frac{w_{r2}\tan\beta_2}{U_2\,\sin\varphi_2}\right)\right)} \qquad (2.3.2)$$

$$D_2 = 2 \times \frac{U_2}{\left(2\times\omega\times\pi/60\right)} \qquad (2.3.3)$$

$$M_2 = \left\{\frac{\left(\frac{U_2}{a_{01}}\right)^2\left[\frac{\left(1-\frac{w_{r2}}{U_2}\tan\beta_2\right)^2+\left(\frac{w_{r2}}{U_2}\right)^2}{1+\left(\left(\frac{U_2}{a_{01}}\right)^2(\gamma-1)\left(1-\frac{w_{r2}\tan\beta_2}{U_2\,\sin\varphi_2}\right)\right)}\right]}{1-\frac{\gamma-1}{2}\left(\frac{U_2}{a_{01}}\right)^2\left[\frac{\left(1-\frac{w_{r2}}{U_2}\tan\beta_2\right)^2+\left(\frac{w_{r2}}{U_2}\right)^2}{1+\left(\left(\frac{U_2}{a_{01}}\right)^2(\gamma-1)\left(1-\frac{w_{r2}\tan\beta_2}{U_2\,\sin\varphi_2}\right)\right)}\right]}\right\}^{1/2} \qquad (2.3.4)$$

Thickness;

$$\frac{b_2}{D_2} = \frac{\left(\frac{\gamma+1}{2}\right)^{1/\gamma-1}\left[1-\left(\frac{D_{1h}}{D_{1t}}\right)^2\right]\left(\frac{D_{1t}}{D_2}\right)^2}{4\left[1+\left(\frac{1+\eta_C}{2}\times\frac{\gamma-1}{2}\times\left(\frac{U_2}{\sqrt{RT_{01}}}\right)^2\sigma_s\right)\right]^{1/\gamma-1}} \qquad (2.3.5)$$

The exit velocity triangle;

$$w_{rz2} = c_{rz2} = \frac{w_{r2}}{\sin\varphi_2} \qquad (2.3.6)$$

$$w_{\theta 2} = w_{rz2} \times \tan \beta_2 \tag{2.3.7}$$

$$c_{\theta 2} = U_2 - w_{\theta 2} \tag{2.3.8}$$

$$c_2 = \sqrt{c_{rz2}^2 + c_{\theta 2}^2} \tag{2.3.9}$$

$$w_2 = \sqrt{w_{rz2}^2 + w_{\theta 2}^2} \tag{2.3.10}$$

$$\alpha_2 = \tan^{-1}\left(\frac{c_{\theta 2}}{c_{rz2}}\right) \tag{2.3.11}$$
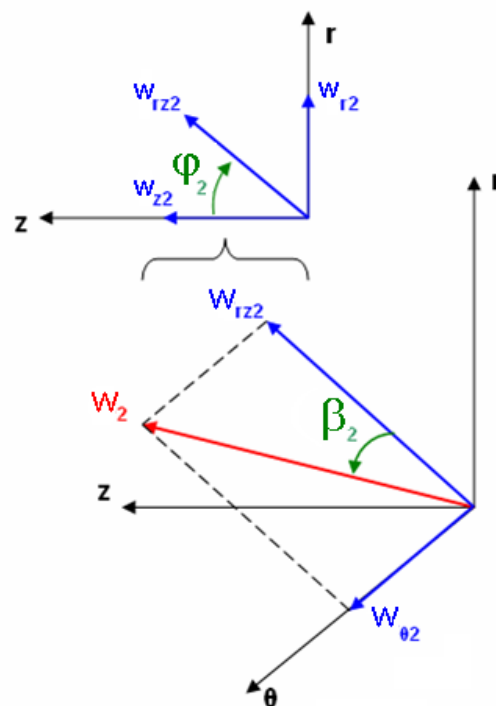
Figure 2.4 – Representation of the velocity triangles at exit

Slip Factor Model; Slip factor is an important issue which has a dominant effect in determining the performance of the impeller. In Paracomp, Stodola

and Stanitz slip factor models [20] are used. Stanitz slip factor is used for radial compressor cases and Stodola is used for mixed flow cases.

Stodola Slip Factor;

$$\sigma_f = 1 - \frac{\pi}{Z}\left[1 - \frac{\sin\beta_2}{\frac{V_{m2}}{U_2}\cot\beta_2}\right] \qquad (2.3.12)$$

These calculations based on Stodola mostly give lower than experimental values, so it may be needed to Stanitz model in order to check the results of Stodola in some cases.

Stanitz Slip Factor;

$$\sigma_f = 1 - \frac{0.63\,\pi}{Z}\left[1 - \frac{1}{\frac{V_{m2}}{U_2}\cot\beta_2}\right] \qquad (2.3.13)$$

Solutions of Stanitz are for the backsweep angle interval of, 45 and 90 degrees. Results match well with experimental values for radial or nearly radial blades.

Inducer Geometry;

$$D_{1t} = 2 \times \frac{U_{1t}}{N \times \frac{\pi}{60}} \qquad (2.3.14)$$

$$D_{1h} = \zeta \times D_{1t} \qquad (2.3.15)$$

$$\dot{m} = \rho_1 \times w_{1m} \times (1 - \zeta^2) \times \left[\left(\frac{D_{1t}}{2}\right)^2 \times \pi \times \cos(\beta_{1m})\right] - \left[\frac{D_{1t}}{2} \times t \times N_b\right]$$
(2.3.16)

20

$$W = \sigma_f \times \left[\left(\frac{U_2}{a_{01}} \times a_{01}\right)^2 - \left(\frac{U_2}{a_{01}} \times a_{01}\right)\left(c_{r2} \times \tan\beta_2\right)\right] \qquad (2.3.17)$$

2.4 Detailed Design

Two and Three Dimensional Design procedure of the Design Algorithm is based on the commercial design program Concepts NREC.

Concepts NREC is a commercial turbomachinery design program, which consists of a group of program modules that are specialized on different turbomachinery types and design phases. In this study three of these modules, named as COMPAL, AxCent and PushButton CFD were used. Compal is a meanline design program for radial turbomachinery which can be explained as improved and graphical supported version of ParaComp. Axcent is a blading program which converts inputs coming from COMPAL to a, three dimensional geometry. Finally, Pusbutton CFD is a CFD solver that works coupled with AxCent, and is able to make two and three dimensional CFD analysis. These three programs constitute a design system which is able to handle a design process from the initial steps until the detailed design phase. In this study this system is used in both database generation and the detailed design parts of the main design algorithm. A detailed explanation of the abilities of these programs is given in the following sections.

2.4.1 Compal

A typical turbomachinery design process invariably begins with meanline calculations. As the initial design of the compressor generated during meanline design phase, this process designates the rest of the design procedure. So that, the success and the rapidness of a design study is closely related with the meanline modeling process. COMPAL is a tool which fills the need of an accurate meanline performance solver, in the current study. It is a commercially available software package which is supplied by Concepts NREC. The program is able to operate in three different modes referred as; design, analysis and data reduction, the last two of which was not used in this study. Design mode is used in order to generate a compressor geometry and predict its performance according to the inputs given by the user. The working screen of design mode of COMPAL is shown in Figure 2.5.
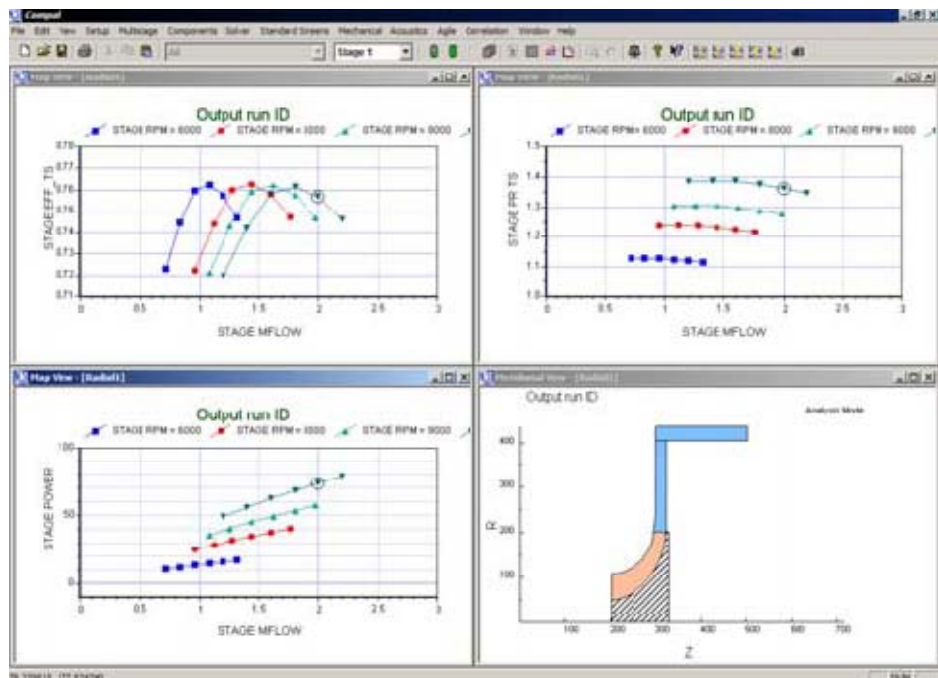
Figure 2.5 – Standart Screen of COMPAL

COMPAL uses a comprehensive set of models to represent the internal physics of the flow and to predict output conditions accurately. A combination of the TEIS (Two Element In Series) and the Two-Zone flow models are the source of this accuracy. Together these models form a One-Dimensional, or meanline, modeling system that represents the basic physics of the flow. The models have several input parameters that must be accurately specified to make reliable predictions. These parameters vary for every machine based on the specific geometry and flow conditions. The models are based on basic geometric and fluid dynamic properties, enabling designers to accurately predict the performance of new designs. As these models are an important part of COMPAL, it is crucial to understand these models in order to use COMPAL effectively and assess the outputs of the program.

2.4.1.1 Two-Zone Modeling;

Two-Zone modeling is a modeling approach that separates impeller exit flow into two regions referred as Jet and Wake. The Jet-Wake phenomena was first shown by detailed flow analysis of Eckardt et al [21] and firstly proposed as a separated flow model by Dean et al [22]. The model improved in years with different investigations the last revisions made by Japikse et al [23].

The Jet and Wake flows are two separated flow regions in the exit of the impeller blade passage. The Jet is approximated as isentropic, while the Wake is a non-isentropic low momentum fluid contained most of the flow losses. The properties of the secondary flow vary with the flow conditions. Japikse [23] also showed statistically that the Two-Zone model yields better performance predictions than those made using similar Level-Two, or so-called Single-Zone modeling techniques.

To complete the Two-Zone model and calculate the change in fluid properties and kinematic parameters, two variables were introduced. First, the ratio of mass flow in the secondary zone to that in the primary zone (χ) must be specified. Second, the exit deviation (δ_{2p}), which is the difference between the exit flow direction and the blade angle, must also be determined. Many correlations have attempted to predict deviation. Wiesner et al [24] presented a review of several common slip factor correlations that can be used for a wide range of machines. In most Two-Zone models, χ is generally assumed to be a constant in the range of 0.15 to 0.25. Use of a constant χ has been considered to be a good assumption, and it is stated in Pelton [14] that, performance prediction was not very sensitive to the specified value of χ.

The Two-Zone model provides designers with an accurate method to predict thermodynamic state change through a radial impeller. To completely specify the output state of the rotor, the kinetic properties of the fluid must also be found. This is accomplished using the TEIS model that provides a simple flow diffusion model of the fluid. By coupling the TEIS model kinetics with the Two-Zone flow thermodynamic calculations, the complete outlet conditions can in theory, be accurately predicted.

2.4.1.2 TEIS Model;

The TEIS model is developed by Japikse et al [25], based on the similarities between impeller flow and the performance of conventional diffusers and nozzles.
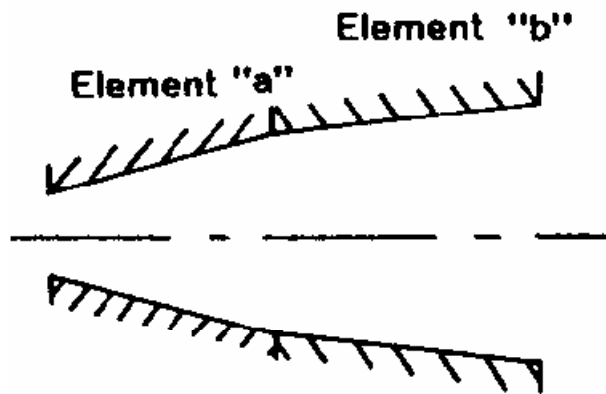
Figure 2.6 – Conceptual representation of the TEIS model showing the
series arrangement of the two flow elements [14].

In the TEIS model, the blade passages of an impeller are modeled
conceptually as two nozzles or diffusers in series, referred to as Elements "a"
and "b" which are shown in Figure 2.6. Element "a" represents the inlet
portion of the blade passage and is considered a variable geometry element
which may either accelerate or diffuse the flow depending on geometry and
mass flow rate. Figure 2.7 shows the basic geometry of Element "a" as it is
used in the TEIS model. In Element "a", the throat area (A_{th}) is constant as

defined by the impeller geometry, but the inlet area (A_{in}) changes with flow
rate. The inlet area is a maximum at high flow rates and a minimum at low
flow rates, as show in Figure 2.7. Therefore, at high flow rate fluid must
accelerate through the inlet and the element acts as a nozzle. Conversely, at
low flow rates the inlet actually diffuses the flow. Element "b" models the
passage portion of the impeller from the throat to the exit of the rotor. For
incompressible fluids, Element "b" acts as a fixed geometry diffuser or
nozzle. For compressible flows the passage portion may function as a
variable geometry diffuser due to the change in density. Figure 2.8 details the
geometry of the passage region.
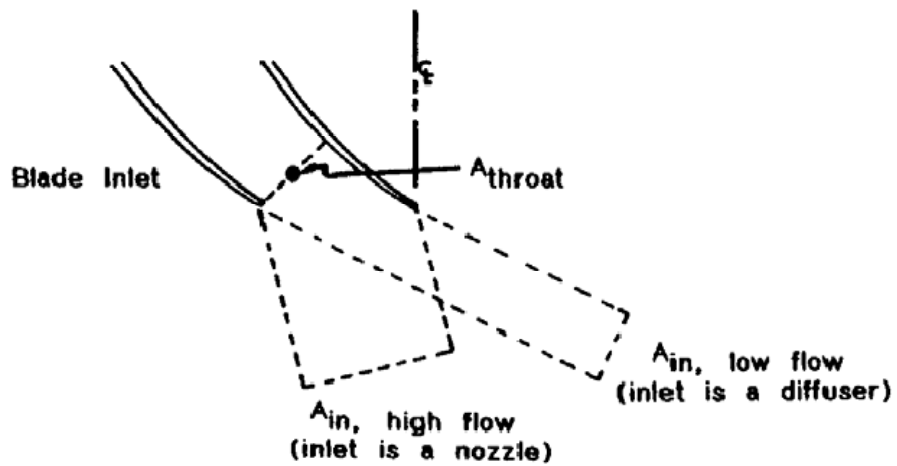
Figure 2.7– TEIS model inlet portion (Element "a") showing variable geometry characteristic of the model [14].
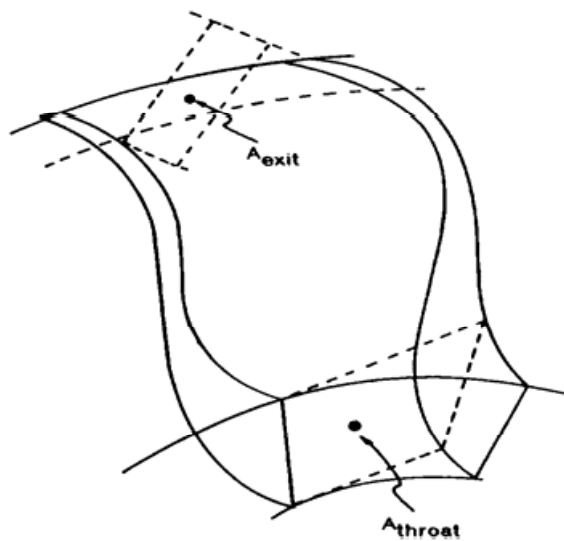
Figure 2.8 – TEIS model passage portion, element "b" [14].

As with diffuser design, the performance of each element may be specified using a corresponding effectiveness value, called η_a and η_b for the inlet and passage elements, respectively. The effectiveness of each element is defined according to a typical diffuser or nozzle effectiveness. The effectiveness of Element "a" is calculated using equation 2.4.1.

$$\eta_a = \frac{C_{Pa}}{C_{Pa,i}} \qquad (2.4.1)$$

In the above expression C_{pa} and $C_{pa,i}$ are the actual and ideal pressure recovery coefficients, respectively. For Element "a" the pressure recovery terms are calculated as follows [14].

$$C_P = \frac{\Delta p}{q} \qquad (2.4.2)$$

$$C_{Pa,i} = 1 - \frac{1}{AR_a^2} = 1 - \left(\frac{cos\beta_1}{cos\beta_{1b}}\right)^2 = 1 - \left(\frac{cos(\beta_{1b}-I_{1t})}{cos\beta_{1b}}\right)^2 \qquad (2.4.3)$$

where q is the dynamic head ($\frac{1}{2}\rho W_{1t}^2$) calculated using the density, ρ, and inlet velocity, relative to the impeller tip, W_{1t}, and Δp is the change in static pressure through the element. AR_a is the area ratio of the inlet to the throat, β_1 is the relative flow angle at the inlet and β_{1b} is the inlet blade angle and I_{1t} is the inlet tip incidence, defined as blade angle minus flow angle

The ideal pressure recovery coefficient shown in equation 2.4.3, is typical of those used in the design of channel diffusers. Japikse [14] comments further on the derivation of this coefficient using Bernoulli's equation, conservation of mass, and its application to diffuser technology. Although in Japikse's derivation, the fluid was assumed to be locally incompressible, the TEIS model is recommended also for compressible fluid systems.

For the passage portion, η_b is calculated in a similar fashion as η_a, shown in equation 2.4.4. C_{pb} is also computed in the same manner as C_{pa} except across element "b", and $C_{pb,i}$ is given by the following Equation [14]:

$$\eta_b = \frac{C_{Pb}}{C_{Pb,i}} \qquad\qquad (2.4.4)$$

$$C_{Pb,i} = 1 - \frac{1}{AR_b^2} = 1 - \left(\frac{A_{th}}{A_{exit}}\right)^2 \qquad\qquad (2.4.5)$$

AR_b is the passage area ratio, A_{th} is the throat area and A_{ex} is the impeller exit area as shown in Figure 2.7. To complete the TEIS model, it is necessary to define the diffusion relative velocity ratio (DR_2) for the overall machine:

$$DR_2 = \frac{W_{1t}}{W_{2p}} \qquad\qquad (2.4.6)$$

Where, W_{2p} is the relative velocity of the primary flow zone at the impeller exit. To extend the range of the TEIS model, the affects of stall must also be accounted for. In general, stall can be roughly approximated using knowledge of the diffusion or pressure loss characteristics of an impeller. In the TEIS model, a constant value of diffusion ratio DR has been used to approximate the effects of stall.

Japikse et al [26] derived the following equation for DR_2^2 to relate the performance model to the output thermodynamic state:

$$DR_2^2 = \left(\frac{1}{1-\eta_a C_{pa,i}}\right)\left(\frac{1}{1-\eta_b C_{pb,i}}\right) \qquad\qquad (2.4.7)$$

Using Equation 2.4.7 in conjunction with Equation 2.4.6, the change in fluid velocity through a rotor can be predicted using η_a and η_b. Furthermore, when

η_a and η_b are known the results can be combined with those from the Two-Zone model and by this way the complete output state of a turbomachinery is modeled in COMPAL.

Matched results are unique to each specific machine and cannot be applied to another geometry or at another flow condition. Early matching results showed a general dependence of η_a and η_b on parameters such as rotor diameter, rotation number, etc. These types of relations suggest that a correlation exists, relating the values of η_a and η_b to the geometry and flow conditions of an arbitrary machine. Japikse et al [26] proposed that a correlation would likely be a function of several geometric and flow parameters, including Reynolds number, a Rotation number, inlet clearance and possibly blade thickness, etc.

There are some flow conditions where the TEIS/Two-Zone model cannot predict performance, including regions of choke or stall. Steady flow usually occurs where the design point is found and where the machine is designed to operate. Since most machines are designed to operate only under conditions of steady flow, it is important to accurately model these conditions. The TEIS model was developed using locally incompressible flow assumptions that work well in stable flow regions even with moderate compressibility. Stall is still a poorly understood phenomenon and in general performance modeling in this realm is not attempted.

2.4.2 AxCent

AxCent is a commercial software package, which completes the design process started with COMPAL, by converting the meanline design to the detailed geometry. AxCent has two main features that makes it capable to manage the detail design process.

In the meanline design, the components of the turbomachine are defined in terms of inlet and exit radii, passage heights, and blade angles at leading and trailing edges. AxCent fills in the details of the blade shape in three dimensions, together with other information, and creates the three dimensional geometry of the impeller design together with the other stage elements as shown in Figure 2.9. As the geometry is generated, it is possible to modify the blade contours, blade angle distribution or thickness manually, according to the preference of the user. The output geometry from AxCent can be used as a starting point for finite element analysis, CFD analysis, computer-controlled machining, and computer-aided drafting tools.

As the design move forward into the three-dimensional geometry generation, it's needed to have enough information about the flow inside the blade passages in order to decide the shape of the geometry. In order to meet this need, AxCent is able to make through-flow and blade-to-blade flow analysis with the solvers embedded into the program. However these solvers give accurate results for subsonic flow conditions only and in this study, as the flow conditions are supersonic, it was not possible to use these tools effectively. Instead, it was preferred to use Navier-Stokes based solvers like Pushbutton CFD in order to have more realistic results.
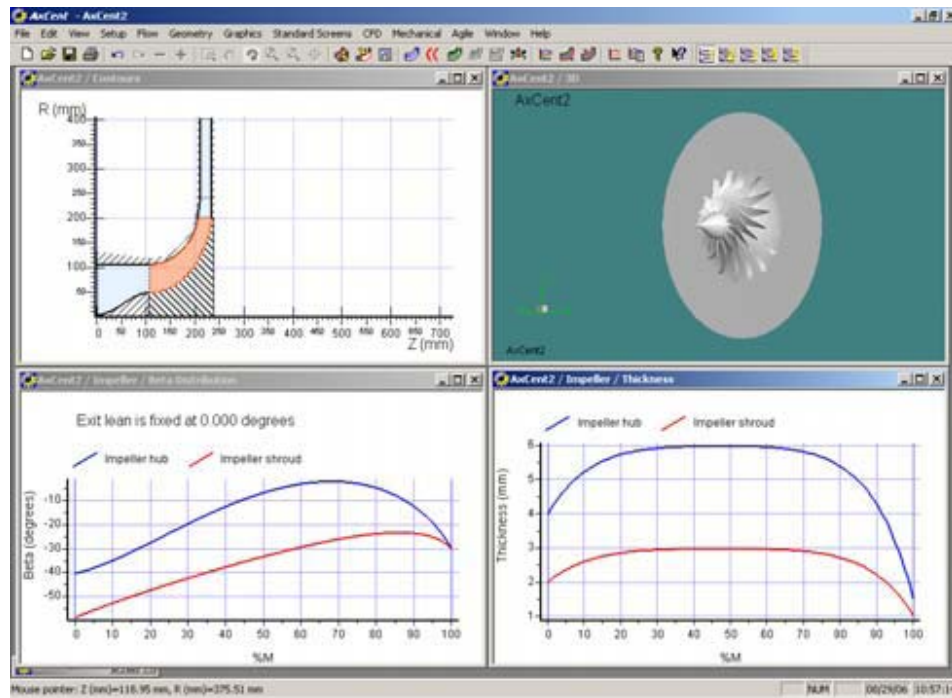
Figure 2.9 – Standart Screen of AxCent

2.4.3 PushButton CFD

Pushbutton CFD is a CFD solver module of Concepts NREC and it works coupled with AxCent. It consists of three CFD solvers: one from Dawes, a Multi-block solver developed independently by Concepts NREC, and a Denton CFD solver.

In this study the Multi-block solver is used, which is also the default solver for Pushbutton CFD calculations. The Multi-block solver is a hybrid multi-block structured grid full Navier-Stokes solver. It can deal with compressible, incompressible, and low speed flow regimes. The Multi-block solver has a central difference scheme as in the Dawes solver. The solver also provides an upwind scheme with first and third orders of accuracy. The governing equations used in this solver are the Reynolds-Averaged full Navier-Stokes equations with Low Mach number pre-conditioning, and Turbulence models

available in the program. Nearly all well known turbulence models are available in the program.

The program has its own mesh generator which is able to create structured grids in required size. However the limiting part of this program is, as it's not a software that is fully focused on the CFD analysis, its grid size, mesh quality and fineness is not as good as a CFD software. In this sense, Pushbutton is a pre-CFD software which gives an idea about the overall passage flow rather than a precise CFD tool.

2.5 Design Of Experiments (DoE)

Design of Experiments (DoE) is a statistical technique for studying the effect of outcome of multiple variables simultaneously. The technique is firstly developed in order to define the robustness as a measure of quality and it's focusing the design process on minimizing the sensitivity of the system to the factors causing variability in performance. There are two tasks to be performed by DoE which are, measurement of Quality during Design or Development and Efficient experimentation to find dependable information about design parameters. These can be achieved by employing the signal-to-noise ratio to measure quality and orthogonal arrays to study many parameters simultaneously. As the purpose of using DoE is generating a reliable database, only orthogonal arrays are used in this study.

Using an orthogonal array is the way of generating the shortest possible matrix of permutations and combinations that gives a well distributed design space [27]. Main characteristics of this method are defined with, the "Balance" and the "Orthogonality". Balance is a concept that, ensures each of the value of a variable is tested in the set of experiments. Likewise

orthogonality ensures equal attention given to each of the combinations of two variables in the same set.

In an orthogonal array, rows consist of variable combinations of each experiment and columns consists of level distributions of parameters. A typical orthogonal array is shown in Table 2.3. In this figure there are four factors named as A, B, C and D. Each factor has three levels, referred as 1, 2 and 3. Normally in this type of a problem, 4 factors can be combined in 4! different ways which is equal to 24. In order to try all of possible cases with 3 different values for each factor, it's needed to make 24^3 = 13824 experiments. However, by using an orthogonal array it's possible to cover the same design space with only 9 experiments. The observation (η) column gives the result obtained from each experiment represented by each row.

Table 2.3– An orthogonal array representation of a Matrix Experiment [28]

Experiment No	Column Number and Factor Assigned				Observation η
	1 A	2 B	3 C	4 D	
1	1	1	1	1	-20
2	1	2	2	2	-10
3	1	3	3	3	-30
4	2	1	2	3	-25
5	2	2	3	1	-45
6	2	3	1	2	-65
7	3	1	3	2	-45
8	3	2	1	3	-65
9	3	3	2	1	-70

Table 2.3 is named as $L_9(3^4)$ in DoE terminology, this means that the array has nine rows and four 3-level columns. Likewise factors with different number of levels may be investigated in the same orthogonal array. In

statistical literature, parameters of the problem are referred as factors and values of these parameters are referred as levels.

The orthogonality of a matrix experiment is an issue, coming from the linear algebra and statistics. Consider 3 observations in Table 2.3 as a result of 3 experiments that are known as, η_1, η_2, η_3 . Consider a linear form L_i, given by equation 2.5.1.

$$L_i = w_{i1}\eta_1 + w_{i2}\eta_2 + w_{i3}\eta_3 \qquad (2.5.1)$$

which is a weighted sum of three observations. The linear form L_i is called contrast if the weights add up to zero- as shown in equation 2.5.2.

$$w_{i1} + w_{i2} + w_{i3} = 0 \qquad (2.5.2)$$

Two contrasts, L1 and L2, are said to be orthogonal if the inner product of the vectors corresponding to their weights is zero.- that is given by equation 2.5.3 and 2.5.4.

$$w_{11}w_{21} + w_{12}w_{22} + ... + w_{13}w_{23} = 0 \qquad (2.5.3)$$

$$[w_{11} + w_{12} + w_{13}][w_{21} + w_{22} + w_{23}] = 0 \qquad (2.5.4)$$

Hence columns 1 and 2 are mutually orthogonal. The orthogonality of all pairs of columns in a matrix experiment can be verified in a similar manner.

To select an orthogonal array, the following steps are to be employed [28],

1. List the number of factors and interactions of interest
2. Decide the number of levels for the factors
3. Calculate the degree of freedom (DoF) for the factors
4. Choose the orthogonal array according to the DoF
5. Prepare the trial data sheet

The Degree of Freedom (DoF) is associated with each piece of information that is estimated from the data. A way of finding the DoF of each parameter is to subtract one from the total number of levels for each. Application of, all of these steps are explained briefly in Chapter 3.

2.6   Optimization Procedure

The optimization process applied in the study is based on the multidirectional search algorithm (MDS) which is an algorithm derived from direct search methods for multivariable nonlinear functions [29].

Direct Search methods are one of the most common application since 1960's. Although the method seems too old, it is not old-fashioned because of its simplicity, robustness and reliability. Direct search is a non-derivative "zero-order" method, which means that, the method does not require derivative information and not construct approximations of the objective function. Although there are also other non-derivative methods, Direct Search distinguishes from these methods with not requiring the numerical value of the function. Thus, it uses the relative rank of the objective values, so that it can accept new iterates that produce simple decrease in the objective. This is in contrast to the convergence conditions for quasi-Newton line search algorithms, which require that a sufficient decrease condition be satisfied. This ability supports the robustness of the method near other higher order relatives [30].

As the method does not require gradient and Hessian information, it is very convenient to apply optimization to a nonlinear function with a simple procedure. Furthermore, the results of the method are reliable enough in case of convergence. Consequently, as the objective function defined in this study is highly nonlinear, Direct Search Method is chosen due to all of these explained features.

Direct Search Methods classified under three main types referred as, pattern search methods, simplex methods and methods with adaptive sets of search directions. Multidirectional Search Algorithm is a patterns search algorithm that is generated in order to remove the weaknesses of Nelder-Mead Simplex Method. The method is based on driving the search by using a simplex like the Nelder-Mead algorithm. Simplex is a set of n+1 points in R^n space, which ensures that any point in the domain of the search can be constructed by taking linear combinations of the edges adjacent to any given vertex [31]. This definition generates a pentachoron, simplex geometry for 5-parameter design space of the current study which is represented in Figure 2.10.
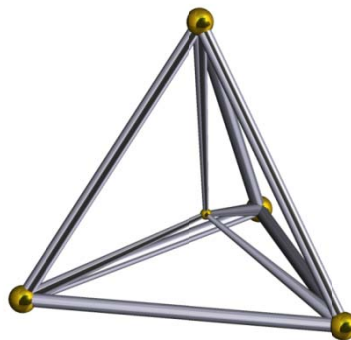
Figure 2.10 – A pentachoron geometry

Figure 2.11 illustrates the two dimensional representation of an MDS algorithm. The algorithm begins with choosing an initial point in design space for constructing a simplex around it (x1, x2 and x3). The vertices on the

simplex are ordered due to the objective function values. As the initial simplex constructed and ordered, second step proceeded by constructing the reflection of the original simplex (x1, r2, r3). If the minimum function value of the vertices of reflection is less than the minimum of original simplex than reflect is accepted and expansion is attempted. The expansion step is, creating a larger simplex on the reflection that has the vertices of x1, e2 and e3. If the minimum value of the expansion is smaller than the reflected simplex, then the expanded simplex is accepted as the new original simplex. Else as the reflected simplex has the minimum function value, it becomes the new original simplex. If none of these happens than it means the original simplex conserves a smaller value than the reflected one. This time the original simplex is contracted and the new simplex having the vertices x1, c2, c3 is identified as the new original simplex.
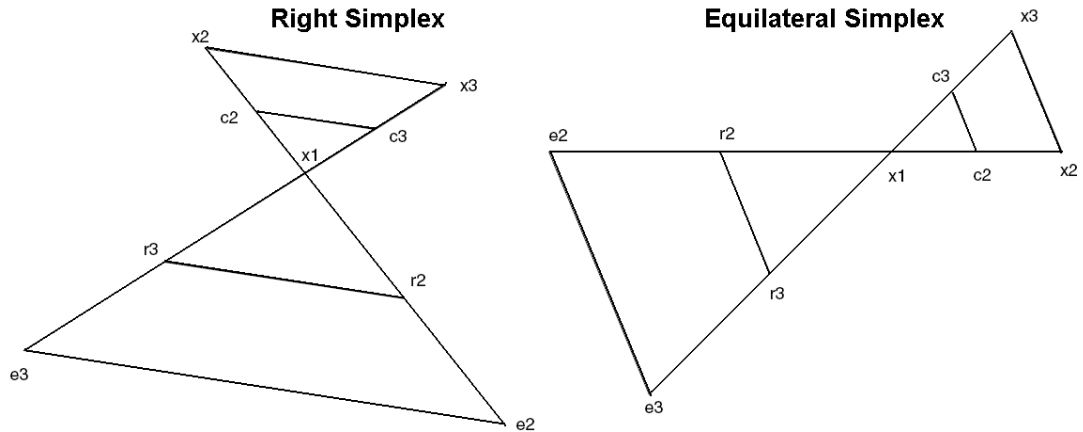
Figure 2.11 – Multi Directional Search Algorithm search path [29]

The pseudo code of the optimization program is given below [29];

1. Evaluate f at the vertices of S and sort the vertices of S
2. Set fcount = N+1
3. While $f(x_{N+1}) - f(x_1) > \xi$
   a. Reflect: If fcount = kmax then exit

      For j=2, ... ,N+1 $r_j = x_1 - (x_j - x_1)$; Compute $f(r_j)$; fcount = fcount + 1

      If $f(x_1) > min_j\{f(r_j)\}$ then goto step 3b else goto step 3c
   b. Expand:

      i.   For j=2, ... ,N+1; $e_j = x_1 - \mu_e(x_j - x_1)$; Compute $f(e_j)$; fcount = fcount+1

      ii. If $min_j\{f(r_j)\} > min_j\{f(e_j)\}$ then

           For j = 2, ... N+1: $x_j = e_j$

           Else

           For j = 2, ... N+1: $x_j = r_j$

      iii. Goto step 3d
   c. Contract: For j = 2, ... N+1: $e_j = x_1 + \mu_c(x_j - x_1)$;compute $f(x_j)$
   d. Sort: Sort the vertices of S

μ_e and μ_c are the coefficients, which determine the size of the expanded and contributed simpleces. It is recommended to give 2 and 0.5 to these parameters, but different values could be given according to the convergence characteristics of the problem [29]. Convergence condition of the MDS algorithm is based on the distance between the vertices. As the simplex shrinks and the difference of vertices becomes less than ξ, the converge condition is satisfied.

Another problem in optimization of a nonlinear function is, the difficulty of finding the global minimum due to the nonlinear and unpredictable structure of the design space. As the design space consumes lots of small hills or local minima-maxima, it is nearly impossible to find the global solution with a single run. In order to solve this problem, the algorithm is modified to an iterated optimization scheme which is based on driving a group of optimization runs started from different initial points and finding global optimum after comparing their results. It takes about 70 runs to find a global optimum point each time in this study.

2.7   Neural Networks

Neural network is a massively parallel distributed processor made up of a simple processing unit, referred as neuron. By the help of its learning capability, it has a propensity for storing experimental knowledge and making it available for use [32]. The concept of neural network is based on two main features called synaptic weights and learning algorithm. Synaptic weight is a key element for storing the knowledge and it gives the parallel computing capability of system by distributing information to different neurons. Learning is a process based on a specialized algorithm which determines the values of synaptic weights. The main advantage of Neural Network is its robustness and rapid data processing capability in very complex problems which is also the reason of its preference for this study.

There are different types of neural networks for various applications. Basically, a neural network is classified according to its structure and the learning algorithm embedded to this structure. A primitive version of this classification is shown in Figure 2.12. Although, the classification of network architecture shows most of the picture in this graph, it is not that much of easy for learning algorithms due to their variety.

39
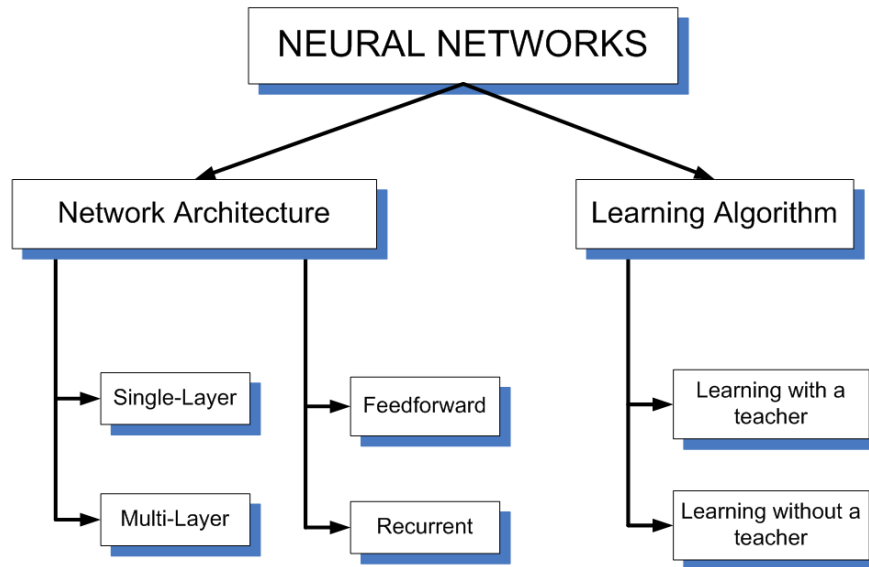
Figure 2.12 – Classification of Neural Networks

The neural network type applied to the current study is, a multi-layer feedforward architecture which uses a learning algorithm that learns with a teacher. An illustration of the architecture of this type of a network is shown in Figure 2.13. The intermediate stages of the structure are referred as hidden layers. Hidden layers are consists of neurons that are in charge of designating weight values.
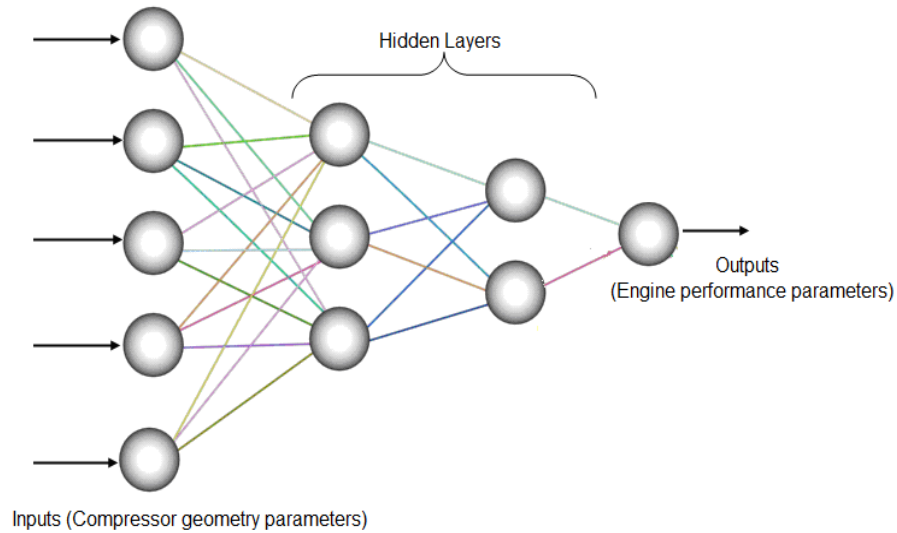
Figure 2.13 – Illustration of Neural Network architecture used in this study

A Neural Network code consists of two parts, referred as trainer that performs the learning process and forecaster that generates outputs according to the weight and bias values determined by trainer. In this distribution, trainer takes the main responsibility about functionality of the system. So that, in order to understand the capabilities of a Neural Network, it is essential to know the learning algorithm that it is based on.

Learning is a process by which the free parameters of a neural network are adapted through a specialized algorithm by then enviroment in which the network is embedded. The type of learning is determined by the manner in which the parameter changes take place. In this study, the learning algorithm of Neural Network code, is based on error-correction learning. Error-correction learning is simply, a type of learning which is driven to find a weight combination that gives the minimum error value. As given in 2.7.1, error value is defined as, the difference of output of the neural network (y_i) and the desired output (d_i) taken from the enviroment.

$$e_i = y_i - d_i \qquad\qquad\qquad (2.7.1)$$

According to this expression, error finding process can be thought as an unconstraint optimization problem which is objected to find the minimum error value by using an iterative search method. Levenberg-Marquardt (LM) algorithm is chosen for this study as search method of the training algorithm. LM is an iterative technique that locates the minimum of a multivariate function that is expressed as the sum of squares of nonlinear functions. The algorithm can be thought of a combination of Steepest Descent and Gauss-Newton method.

As the weight combination that gives the minimum error is found, it is placed in the output formulation given in 2.7.2. According to this expression, output of function f is determined by, putting input (x_i), weight (w_{ki}) and the bias (b_k) values into the formula. This is a linear neuron expression which can also be turned into a nonlinear expression according to the type of application, by some modifications. The illustration of the information flow that gives the formulation in 2.7.1 and 2.7.2, is shown in Figure 2.14.

$$y_k = f\left(net_n\right) = f\left(\sum_{i=1}^{m} w_{ki} x_i + b_k\right) \qquad (2.7.2)$$
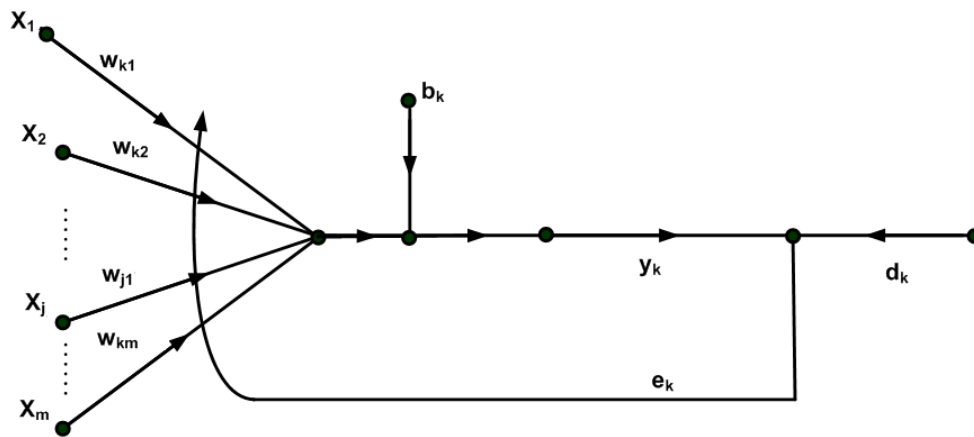
Figure 2.14 – Illustration of Neural Network information flow structure on one neuron [32]

As stated before, Neural Networks can be used for different purposes as well as a function approximator like in this study .In the current methodology, the inputs of Neural Network trainer is combined with the designs generated due to the matrix which comes from Taguchi's DoE method [33]. By putting the model generated from the trainer into the forecaster it is obtained a function that defines the design space. Later on the forecaster is embedded to the optimization code and the generation of model needed to drive the optimization process is completed by this way. The settings and the results of the whole algorithm is briefly given in Chapter 3.

CHAPTER 3

MIXED-FLOW COMPRESSOR IMPELLER DESIGN

3.1 Performance Characteristics of a Mixed Flow Compressor

The main advantage of mixedness in a centrifugal compressor is the mass flow rate increment with decreasing meridional exit angle from 90 degrees. This feature could be represented by using the kinematic characteristics of the exit flow which is illustrated in Figure 3.1.
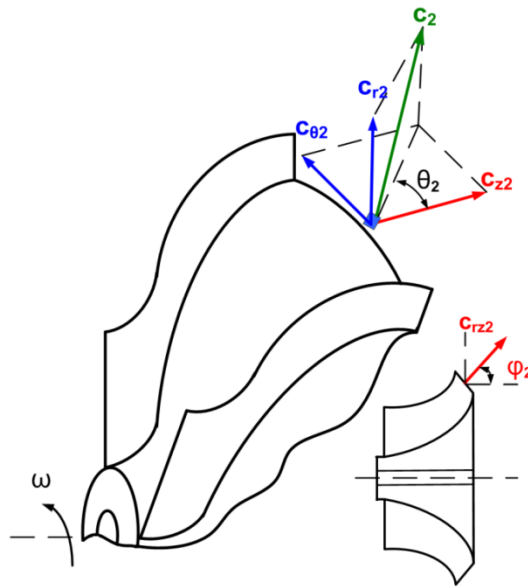
Figure 3.1 – Illustration of exit flow components of a mixed flow compressors

Apart from the radial compressor, meridional exit angle (φ_2) creates an axial velocity component (c_{z2}) that produces a two dimensional component in rz

plane (c_{r2}) by combining with the radial velocity component (c_{r2}) as given in 3.1.1 .

$$c_{rz2} = c_{r2} + c_{z2} \qquad (3.1.1)$$

Thus by the addition of the axial velocity component the expression of the flow coefficient, is modified as given in the equation 3.1.2. As the radial and axial components are related according to the equation 3.1.3, the flow coefficient can be expressed by using this equation .

$$\phi = \frac{c_{rz2}}{U_2} \qquad (3.1.2)$$

$$\frac{c_{z2}}{c_{r2}} = \frac{c_{z2} \cos \varphi_2}{c_{z2} \sin \varphi_2} = \frac{1}{\tan \varphi_2} \qquad (3.1.3)$$

$$\phi = \left[1 + \frac{1}{tan \varphi_2} \right] \frac{c_{r2}}{U_2} \qquad (3.1.4)$$

As c_{r2} = w_{r2}, equation 3.1.4 turns into;

$$\phi = \left[1 + \frac{1}{\tan \varphi_2} \right] \frac{w_{r2}}{U_2} \qquad (3.1.5)$$

According to the expression in 3.1.5, flow coefficient increases with a decrement in meridional exit angle, so this means that mass flow rate of a mixed flow compressor is higher than a radial compressor under same conditions. If this expression is embedded into the pressure ratio equation

which is determined from Euler Turbine and Energy Equations then the formula given in 3.1.6 is obtained.

$$\pi_c = \left[1 + \eta_c(\gamma - 1)\left(\frac{U_2}{a_{01}}\right)\frac{\tan\varphi_2}{\sin\theta_2}\frac{w_{r2}}{U_2}\right]^{\gamma/\gamma-1} \qquad (3.1.6)$$

In contrary with the flow coefficient, equation 3.1.6 shows that as the meridional exit angle increases, pressure ratio of the compressor decreases with constant dimensions and under the same operating conditions. Both the behavior of pressure ratio and mass flow coefficient extracted from given expressions is represented in Figure 3.2.
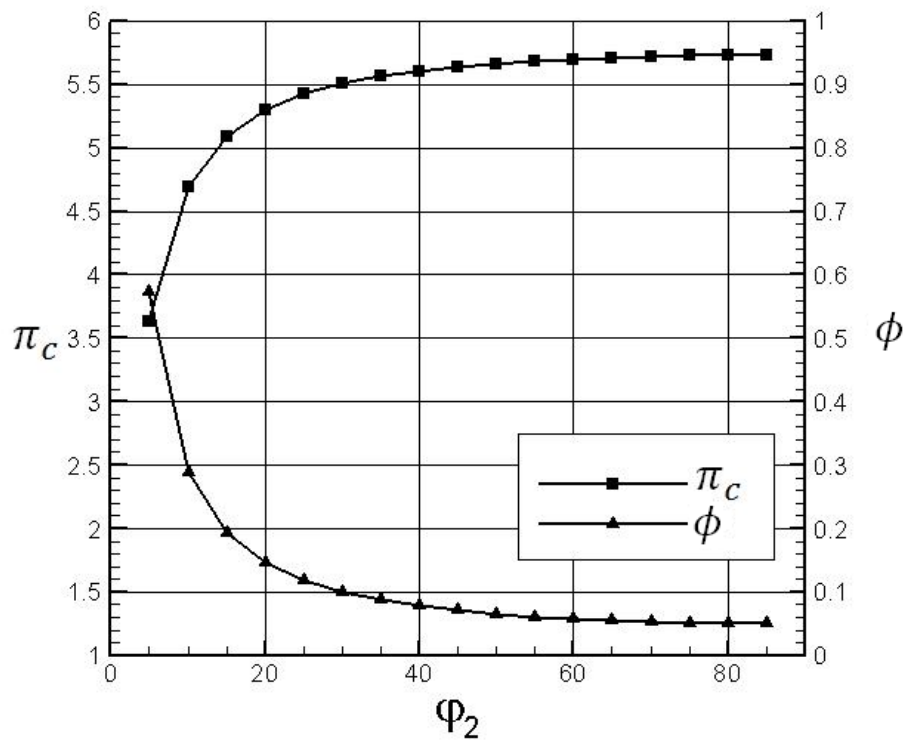
Figure 3.2 – Variation of the pressure ratio and flow coefficient with meridional exit flow angle (φ_2)

46

Figure 3.2 clearly shows that meridional exit angle is a parameter that increases the mass flow capacity if a compressor turns into a mixed flow from purely radial flow at exit. However, opposite tendencies in pressure ratio and mass flow rate causes a dramatic decrement in pressure ratio which is unfavourable for the current design case. This inappropriate situation shows that, pressure ratio should be kept in a reasonable level for engine performance and it is focused on, to increase the mass flow under this condition.
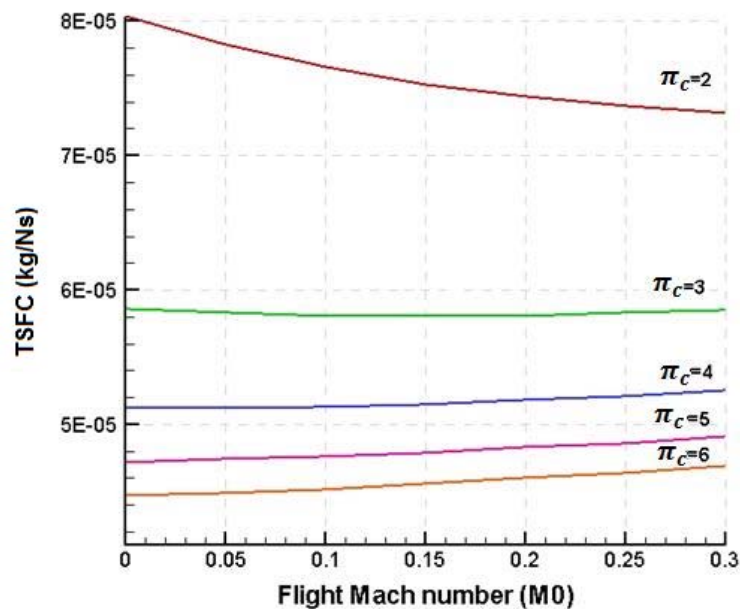
Figure 3.3 – Effect of pressure ratio to TSFC in a small gas turbine engine design

In order to reach this goal, compressor behavior is investigated by restricting the pressure ratio. Due to the phsical necessity born from this regulation, the power input of the compressor is relaxed. To decide an appropriate level for pressure ratio, different engine combinations are generated by using the engine design code. According to the fuel consumption trends shown in Figure 3.3, it is obviously seen that pressure ratio of 5 is a suitable setting, in

order to get maximum gain from the engine performance with a reasonable effort.

With these new arrangements, the behaviour obtained from the designs generated by using Compal, is shown in Figure 3.4. It can be seen from the figure that, it is possible to obtain the expected behavior of mixed flow compressors while keeping the pressure ratio in a reasonable level. But there is an important dillema that is arisen from the increment in power consumption proportional with the mass flow rate as shown in Figure 3.5.
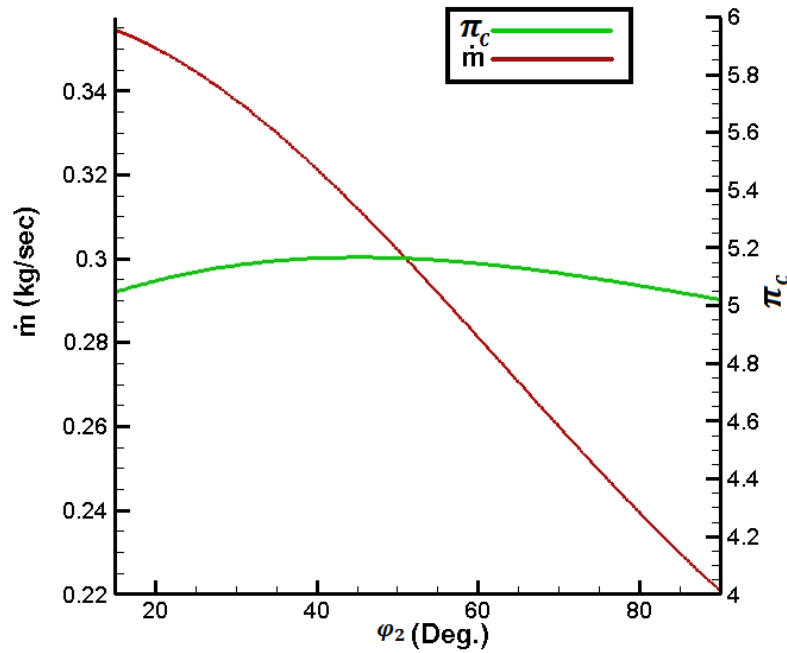
Figure 3.4 – Variation of mass flow rate with meridional exit angle according to the restricted pressure ratio.
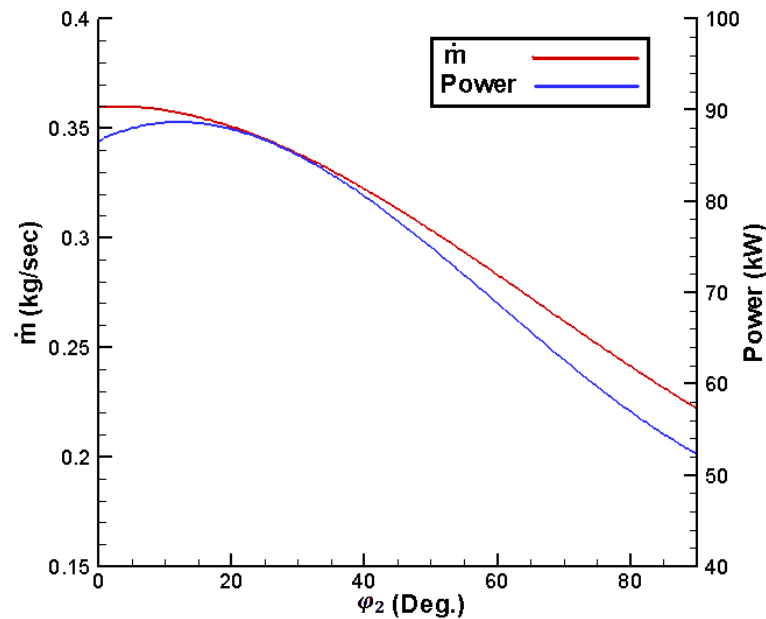
Figure 3.5 – Variation of power and mass flow rate with meridional exit angle

However as the problem is not only limited with the compressor design considerations, but also the effect of compressor to the engine is an important factor that shapes the problem. So it is also needed to take care the thrust gain with respect to the consumed power. In order to parametrize this characteristic, thrust to power ratio is defined which shows the thrust generated by the engine with respect to the power consumed by the compressor. The change of thrust to power ratio and power consumption with respect to the mixedness is shown in Figure 3.6. As can be seen from this figure, thrust gained per kW is decreasing with the decreasing meridional exit angle. Therefore, it is possible to say that, giving mixedness to a centrifugal compressor is a feasible application in order to increase the performance of a gas turbine engine. However, it should be noticed that all engines have a power supplement capacity determined by turbine design and energy extraction at combustion chamber. According to this situation, the power consumption brings out an important limitation for the design, which turns the deisgn case into an optimization problem.

49
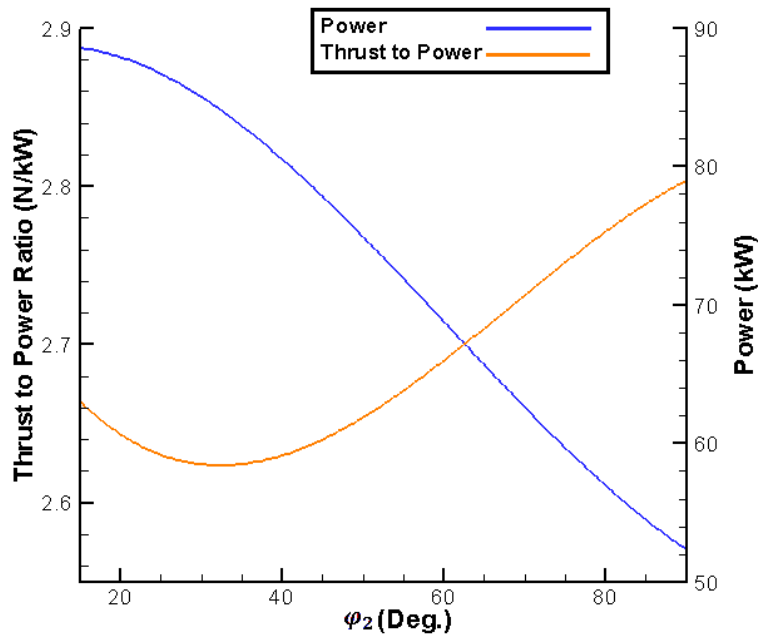
Figure 3.6 – Variation of thrust to power ratio and power consumed by the compressor with meridional exit angle

Since the applicability of mixed flow compressor for more mass flow requirement seems feasible, the next step is to determine the appropriate meridional exit angle for a defined problem. It is seen from Figure 3.4 that as the meridional exit angle decreases the performance becomes more favourable. Nevertheless as this chart doesn't give any sense about the performance expactations of the engine, it is needed to look at the effects of compressor performance on the engine performance. Figure 3.7 is a chart that consists of Engine performance versus meridional exit angle data, derived from the compressor performance characteristics by using the engine design code. Engine performance is represented by Thrust Specific Fuel Consumption and Specific Thrust in the graph. The figure shows that, both of the performance parameters has a distinct and nonlinear behavior with the variance of mixedness. This circumstance is the second factor which, forces the designer to handle the study as an optimization study in order to find the suitable mixedness angle that gives the desired performance. As the

compressor performance is a phenomena that is shaped according to the close interaction of different design parameters, it is not possible to make a realistic optimization study by using only one parameter. So this well known circumstance reshape the optimization problem by adding the compressor design parameters near the meridional exit angle.
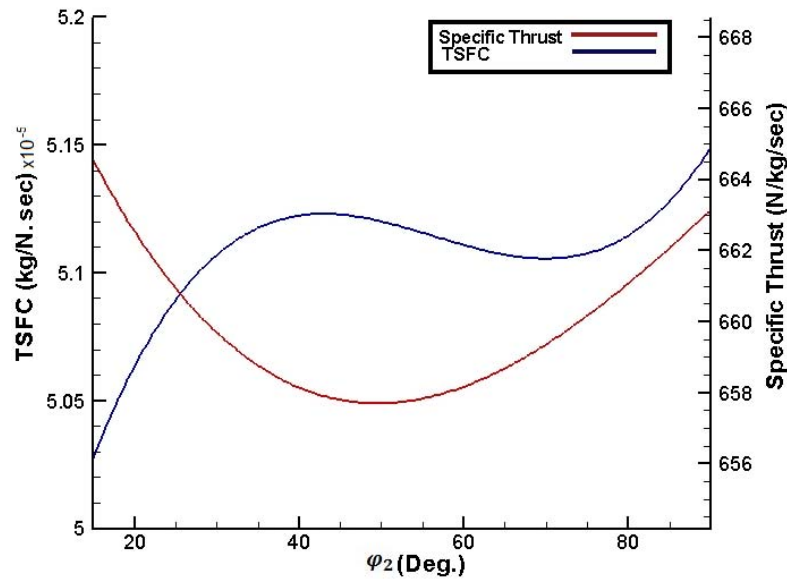
Figure 3.7 – Variation of Thrust Specific Fuel Consumption (TSFC) and Specific Thrust with meridional exit angle.

Consequently, it is understood that mixed flow compressors are suitable for a small gas turbine design from the performance point of view. According to this result , the design algorithm explained in chapter 3 is applied in order to design a mixed flow compressor for a small turbojet engine. The procedure followed in this study is explained briefly including results, in following parts of chapter 3.

3.2 Engine Design Case

The first step of the methodology is to determine the performance needs of the compressor according to an engine design case by computing the engine cycle. This is done by using engine design code which is explained in detail in chapter 3.

The requirements of the engine are set as 220 N thrust and 0.3 Mach flight Mach number at sea level. These requirements are derived from performance data of various small air vehicles found from literature [10]. As a design limitation, fuel type is selected as JP-8. Component figure of merits are taken according to the trends in these types of engines. Burner pressure ratio is taken as 0.9, Mechanical efficiency of the engine is 0.95 and burner efficiency is 0.9.Burner efficiency may be taken as small as 0.8 for a small gas turbine engine. T_{t4} is taken as 1400K which is actually a high value for a single stage axial turbine without any cooling. But it has shown that in TJ-50 engine of Hamilton-Sundstrand, by using ceramic alloy for turbine, it is possible to reach this value for a 30 minutes working engine [10].

The last value needed to be determined is the pressure ratio, which is found iteratively and chosen according to some limitations given by the user. The main limitation in this design is the power consumption of the compressor that is set as 90 kW. The results of the cycle code is given in Table 3.1, these results also shows the reference performance requirement of the compressor. According to this data, the initial design is shaped in order to give 4.8 pressure ratio with 0.36 kg/s mass flow rate and 0.75 isentropic efficiency. The engine and compressor performance determined at this step may seem too optimistic, especially 4.8 pressure ratio is too high for this size of a radial compressor. But as it is wanted to show the variation of the design data through the methodology, this kind of an optimistic engine alternative is

selected. In following steps this data will modified to more realistic values according to the more detailed results.

Table 3.1 – Results of the one dimensional engine design code

Symbol	Value	η Compressor	0.753
M_0	0.3	η Turbine	0.815
π_C	4.8	π_t	0.432
T_{t4}	1400 K	τ_t	0.858
Thrust	220 N	τ_c	1.752
$\dot{m}_0$	0.363 kg/s	M_{exit}	1.0
$\dot{m}_{fuel}$	0.0123 kg/s	$W_{turbine}$	94.5 kW
P_9/P_0	1.0865	$W_{compressor}$	85 kW

However, the general performance of the engine is not that much of optimistic. For instance, the total efficiency of engine is found as 0.042, which is extremely low for a regular gas turbine engine, but not that much of vital for a small expandable turbojet. The same inefficiency can be seen in compressor and turbine also. These inefficiencies are also an important measure that causes to exclude the efficiency from cost function in optimization problem.

3.3 One Dimensional Design Of The Compressor

After setting on design performance, the size and the design rpm value of the compressor needed to be determined in order to have some reference values before the detailed design. As explained in chapter 3, a one dimensional in-house design code called ParaComp is used for this purpose. The goal of this step is, having a general idea about the size in order to start the detailed design. The results taken from the ParaComp according to the inputs from

previous step, is given in Table 3.2. The user-defined inputs of the code are, pressure ratio, mass flow rate, rotational speed, blade number, backsweep value (β_2) at the exit, meridional exit angle (φ_2) and isentropic efficiency.

Normally because of the difference between the exit geometry, mixed flow compressors have greater penalty about the diameter. However as one of the goals of this study is to show the advantage of mixed flow compressors to radial ones, the diameter is designated according to size trend of this kind of a purely radial compressor by setting meridional exit angle as 90 degrees. The rotational speed is also set by looking at on-design speed of these type of engines which varies between 100 and 130 krpm. On the other hand, backsweep angle is set by trying different values, which gives a reasonable value for diameter, pressure ratio and mass flow rate.

Consequently, the combination which gives a reasonable performance-geometry combination is fixed as preliminary design of the impeller. As this configuration put is into Compal in order to start the detailed design, these values are also validated by a more precise tool. By determining the reference geometry, adequate number of information is gathered in order to build up the optimization problem.

Table 3.2 – Results of the one dimensional design code ParaComp

Performance		Geometry	
M_0	0.55	Tip Diameter (mm)	86
$M_{1relative}$	1.1	R_{1h}/R_{1t}	0.33
Mass Flow Rate (kg/s)	0.38	D_{1t} (mm)	55
Pressure Ratio	5	D_{1h} (mm)	18
Rotational Speed (rpm)	120000	B_2 (mm)	5.5
Isentropic Efficiency	0.753	Blade Number	7
Power (W)	90000	Impeller Length (mm)	37
M_2	1.2	$Beta_{1t}$ (deg.)	-58
Slip Factor	0.85	$Beta_2$ (deg.)	-18

3.4 Optimization Problem

After obtaining the initial configuration of the compressor, all the data needed to construct the optimization problem is obtained. Problem setting is the first part of optimization study which is followed by establishing function that models the behavior of the system and finding the optimum solution by using an optimization technique. An optimization problem consists of three elements, which are cost or objective function, decision variables and constraints. The cost function has priority between the others, as it defines other two factors in the problem. Cost function consists of specific thrust and thrust specific fuel consumption that are two important parameters that defines the performance.

Cost function is a simple linear formula which is given in 3.4.1, constants A and B are arbitrary constants between 0 and 1, which shows the importance of the parameter relative to other. Cost function is related inversely proportional with specific thrust and directly proportional with thrust specific fuel consumption (TSFC). In this case, the maximum value of specific thrust

and the minimum value of TSFC direct cost function to the minimum value so that the optimization is a minimization study. Both of the parameters are normalized due to their maximum and minimum values in order to remove the difference coming from diversity coming from units of two parameters.

$$COST = (A \times Specific\ Thrust^{-1}) + (B \times TSFC) \tag{3.4.1}$$

$$0 > A, B > 1$$

$$A + B = 1$$

Decision variables are assigned due to the influence (sensitivity) of each variable on objectives and constrained quantities. There are two types of variables according to this classification, referred as high sensitivity and moderate or low sensitivity variables. High sensitivity variables are the variables which produces great modifications on performance with small variations. For this study, as the criteria for the performance of a compressor is mass flow rate and pressure ratio, the measure of sensitivity becomes effect of a parameter on these features. According to this definition, high sensitivity variables determined from the literature are, impeller tip diameter, meridional exit angle, backsweep angle, tip depth, inducer inlet angle (or rotor incidence) and rotor eye [15]. The moderate-sensitivity variables which determined in same way are, blade leading shape, some curvature parameters of the blade shape and tip clearance [15]. In this study only some of the parameters with high sensitivity and none of the moderate sensitivity parameters are taken into consideration according to the given explanations;

First of all, since the study is based on a parametric design instead of blade geometry tailoring, it is unfeasible to study on the curvature and the leading edge shape. Although Leading edge shape is an important design parameter for structural and vibrational design, structural and vibrational considerations are not involved by this study. Likewise, tip clearance is also a parameter which is not taken into the problem, due to the small size of the compressor.

As the size of a compressor gets smaller, inefficiency due to the tip losses becomes something inevitable for the design. Though, the efficiency gained from the modifications makes so little sense on performance that, it brings out so much effort for a little gain.

Consequently, five decision variables are remained for the problem which are, blade exit angle (β_2), Blade tip depth (b_2), Incidence angle (i), Rotor inlet diameter ratio ($\zeta = r_{1h}/r_{1t}$) and rotor meridional exit angle (φ_2). The incidence angle is used instead of blade inlet angle because it's possible to set inlet angle distribution by using incidence. The rotor inlet diameter is represented by the ratio of tip and hub diameters. Likewise, the blade height is represented by ratio of blade heights at inlet and the exit (b_2/b_1) which makes sizing the compressor more practical during the design.

Backsweep, has a significant positive effect on the efficiency and the operating range of the compressor. Backsweep also makes diffuser design easier, however these beneficial effects compensated by increasing peripheral stresses. The role of incidence is critical for both efficiency and the operating range. As the design case of this study is based on a transonic compressor design, incidence becomes more critical because of its narrow operating range. The design value of the incidence does not show the real incidence especially for the off-design conditions but it is used as a tool which sets the inlet blade angle distribution. The rotor eye is one of the key feature that determines the mass flow passing through the compressor, inlet velocity and inlet swirl distribution. These features determine the mass flow that is available to energize during moving through the passage. The inlet passage area also determines the usage of splitter blades which enhances the performance in case of increasing operating mass flow rate. As long as the primary goal of this problem is, to determine the effect of compressor design to the engine performance the selected parameters are enough to build up a model.

The last part of an optimization problem consists of designating constraints, which ensures the consistency of the problem with the physical conditions. There are four constraints determined for the model two of which are equality and other two are inequality constraints. Equality constraints are external diameter and rotational speed and other two inequality constraints are Operating Range and Power consumption.

Impeller tip diameter is the main constraint of this problem which also restricts the pressure ratio. According to this arrangement, impeller tip diameter value set as 86 mm according to the knowledge coming from similar compressor designs. The other equality constraint is rotational speed which is set as 120000 rpm. Although it seems too high from the structural point of view, TJ projects of Hamilton Sundstrand shows that it is possible to build an engine that can handle a shaft speed at this level. The inequality constraints, Operating Range and Power consumption are set as 95 kW and 0,75. Power is the allowable upper limit, considering the total inlet temperature and diameter of the turbine. Power limit is determined by some design trials for single stage axial turbine working in determined T_{t4} and rotational speed values. Operating range is defined in 3.4.2 where the reference mass flow is taken from the choke condition instead of stall limit.

$$OR = \frac{\dot{m}_{operating}}{\dot{m}_{choke}} \tag{3.4.2}$$

In the definition of operating range, it is more usual to see stall mass flow rate instead of choke because of the general trend about designing more efficient compressor by pushing the stall limit. However as the problem is focusing on performance of the compressor rather than efficiency, it is more useful to make the definition by choke limit.

As a result, the optimization problem is defined as; "*Given design values of impeller radius and rotational speed, minimize cost function at the design point by modifying the decision variables. Ensure OR < OR_{max} and Power < $Power_{max}$*"

3.5 Determining Database by Using Design of Experiments

As mentioned before, Design of Experiments (DoE) is a technique for studying the effect of outcome of multiple variables simultaneously. Further information about Design of Experiments is briefly given in chapter 2. Again in chapter 2, it is given a step by step procedure to generate a data base, in this study that procedure is employed in given order.

As the Taguchi's method applied to the optimization problem it has seen that there are five control factors in the problem. It is decided to divide each factor into five distinct levels in order to investigate their behavior in entire design space. The list of factors and their levels distributed to each factor can be seen from Table 3.3.

Table 3.3 – Table of Control Factors and their levels

CODE	FACTOR	Level 1	Level 2	Level 3	Level 4	Level 5
A	φ_2, (°)	15	30	45	60	90
B	β_2, (°)	0	10	20	30	40
C	ζ	0,15	0,2	0,25	0,3	0,35
D	Incidence, (°)	-1	-0,5	0	0,5	1
E	b2/b1	0,2	0,25	0,3	0,35	0,4

Consequently, it has seen that the total value of Degree of Freedom (DoF) is 5 x (5-1) +1 = 21. This means that, there must be at least 21 experiments needed in order to generate a model for this problem. according to this

information the orthogonal table must have at least 21 number of rows in order to represent whole design parameters equally and distribute them homogeneously in design space.

According to the DoF value, the standard orthogonal array for this problem is determined as $L_{25}(5^6)$ table between 18 standard orthogonal arrays [8]. $L_{25}(5^6)$ array has 25 rows and 6 five level columns, which can be seen in Table 3.4. Last column referred as F, didn't used in the study due to having 5 factors in the problem.

Table 3.4 – Orthogonal array L$_{25}$(5^6) layout for experimentation [31]

Experiment #	A	B	C	D	E	F
1	1	1	1	1	1	1
2	1	2	2	2	2	2
3	1	3	3	3	3	3
4	1	4	4	4	4	4
5	1	5	5	5	5	5
6	2	1	2	3	4	5
7	2	2	3	4	5	1
8	2	4	5	1	2	2
9	2	4	5	1	2	3
10	2	5	1	2	3	4
11	3	1	3	5	2	4
12	3	2	4	1	3	5
13	3	3	5	2	4	1
14	3	4	1	3	5	2
15	3	5	2	4	1	3
16	4	1	4	2	5	3
17	4	2	5	3	1	4
18	4	3	1	4	2	5
19	4	4	2	5	3	1
20	4	5	3	1	4	2
21	5	1	5	4	3	2
22	5	2	1	5	4	3
23	5	3	2	1	5	4
24	5	4	3	2	1	5
25	5	5	4	3	2	1

Table 3.5 – Final trial data sheet and the cost value obtained for each design

Design #	φ_2 (°)	β_2 (°)	ζ	Inc (°)	b_2/b_1	Cost
1	15	0	0,15	-1	0,2	9,36
2	15	10	0,2	-0,5	0,25	10,90
3	15	20	0,25	0	0,3	14,21
4	15	30	0,3	0,5	0,35	20,56
5	15	40	0,35	1	0,4	29,14
6	30	0	0,2	0	0,35	9,76
7	30	10	0,25	0,5	0,4	10,57
8	30	30	0,35	-1	0,25	32,63
9	30	20	0,35	1	0,35	16,54
10	30	40	0,15	-0,5	0,3	30,78
11	45	0	0,25	1	0,25	10,00
12	45	10	0,3	-1	0,3	15,13
13	45	20	0,35	-0,5	0,35	21,33
14	45	30	0,15	0	0,4	20,53
15	45	40	0,2	0,5	0,2	41,45
16	60	0	0,3	-0,5	0,4	15,21
17	60	10	0,35	0	0,2	14,14
18	60	20	0,15	0,5	0,25	18,57
19	60	30	0,2	1	0,3	28,38
20	60	40	0,25	-1	0,35	63,86
21	90	0	0,35	0,5	0,3	20,56
22	90	10	0,15	1	0,35	22,17
23	90	20	0,2	-1	0,4	40,97
24	90	30	0,25	-0,5	0,2	51,09
25	90	40	0,3	0	0,25	176,90

By replacing the level numbers in Table 3.4 with the real values the trial data sheet shown as Table 3.5, is generated. After this, the next step is generate each design, that is showed by the trial data sheet. Every row in the trial data sheet meets with a compressor design in the problem. For example, the first row in Table 3.5 represents a mixed flow compressor with 15 degrees meridional exit angle with 0.15 inlet radius ratio and 0.2 blade height ratio, a inlet beta distribution according to the -1 incidence and a radial blade exit. As a result, 25 different compressor designs shown by the data sheet is generated by using the Compal module of NREC. Although in this study, this step is applied by using a design code it is also possible to put some experimental data to each row which will also increase the precision of the results.

At last step, compressor design point performance data which is extracted from designs generated according to the trial data sheet, is converted into engine performance parameters by using the engine design code. The cycle code has driven by only changing the pressure ratio and the mass flow rate and setting T_{t4} value constant. This step is actually transferring the design space of the problem from the compressor performance base to the engine performance base. Graphical representation of engine performance based design space is represented in Figure 3.8.
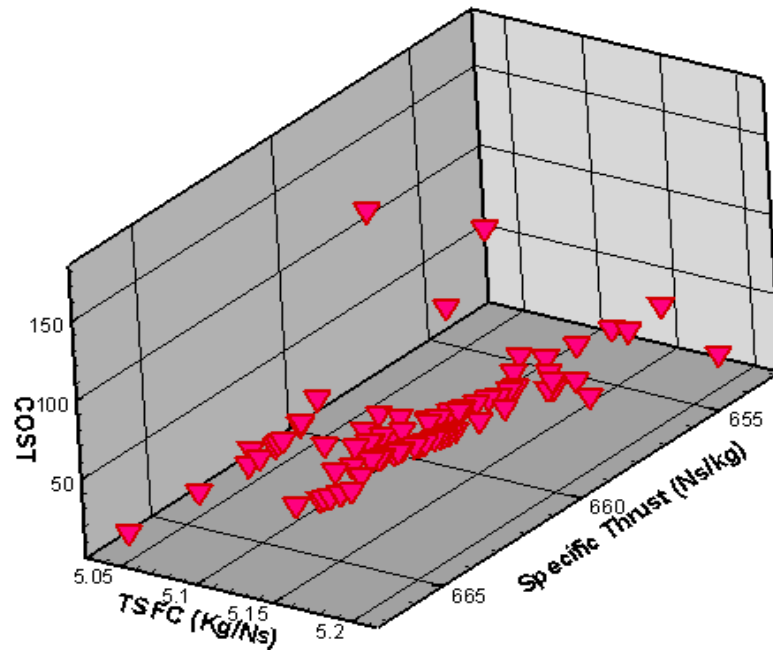
Figure 3.8 – Representation of the design space with 100 samples based on engine design parameters

The goal of DoE is to give the minimum number of samples needed to represent whole design space. However it is possible to extend this sample space due to the capability of the designer. As the number of samples increase it's possible to obtain a more precise results from the Neural Network. So that in order to improve the reliability of the DoE results and increase the precision, the number of samples increased to 100 instead of 25. These 75 additional samples didn't determined from a specific method like DoE, but they are generated by considering a homogeneous distribution in the design space. As a non-homogenity in the distribution of samples in the design space may cause a bias error in Neural Network, the results of both 25 and 100 sample databases are compared and a slight difference has seen between the results. As the 100 sample database has given more precise results, the weight and bias values of this results is used. Difference of cost function variation in both of the databases can be seen from Figure 3.9 and Figure 3.10.
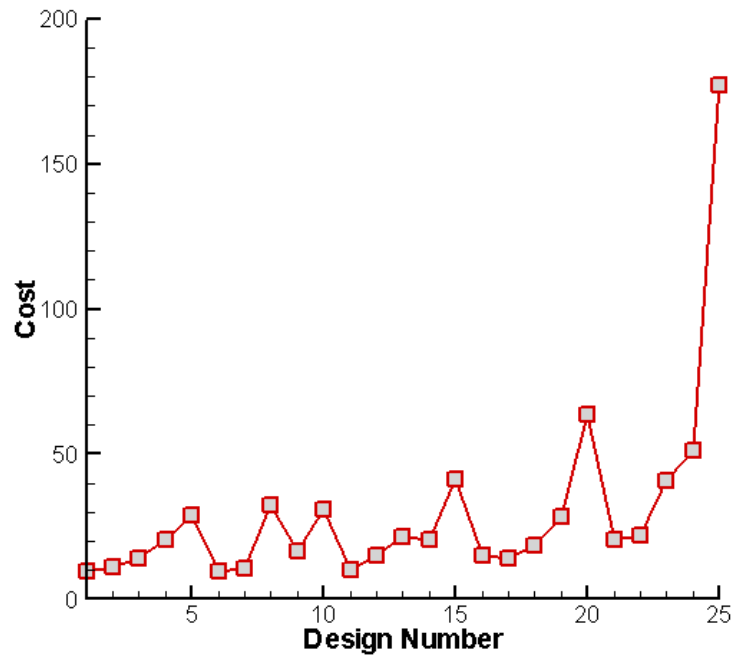
Figure 3.9 – Cost function generated from the engine performance data of the database with 25 samples
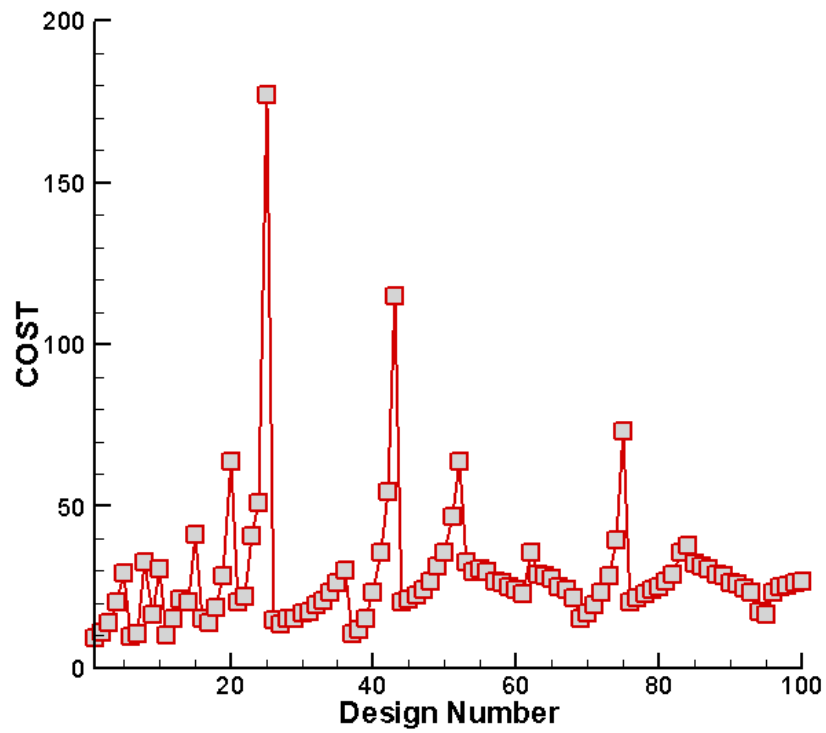
Figure 3.10 – Cost function generated from the engine performance data of the database with 100 samples

Determining the cost values for each database element is the end of database generation. The resulting cost values and decision parameter combinations which gives the design of these costs are used as an input for the training process of the Neural Networks study that will be explained in the next step.

3.6 Neural Networks

Neural Networks is used as a function approximator in this study, which is using the information coming from the database in order to model the design space. The reason of the selection of this method and its capabilities are given briefly in Chapter 3.

Neural Networks code, driven with five inputs according to obtain two outputs which are the cost function and the power. The cost and power values obtained from the database is given to the trainer as target values and it is expected to generate a weight-bias set by using these input and target values.

Training Network is constructed on 2 hidden layers, which includes 5 neurons in the first and 10 neurons in the second hidden layer. Computation time takes a couple of minutes for convergence to a steady state error (SSE) of 10^{-3} order. The convergence characteristics of SSE is given in Figure 3.11 and it is defined as the total of the squares of the error of each training sample. In order to increase the precision of Neural Networks cost parameters are enlarged 10 times to the original values. So that by looking at the range of cost values which changes between 10 and 40 with this modification, it is possible say that 10^{-3} error is a good approximation to the real data.
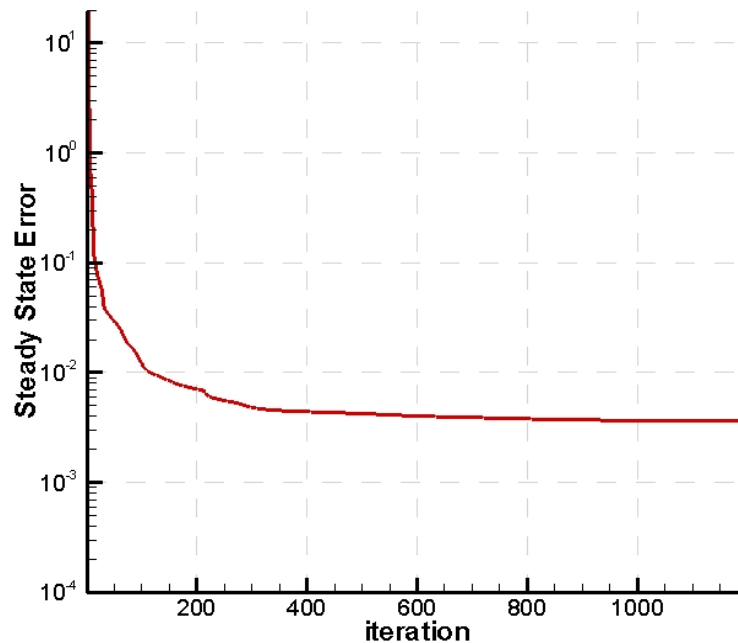
Figure 3.11 –Training trend of the Neural Network in the present study

The weight and bias values generated by the trainer is taken into the forecaster, which generates outputs for arbitrary inputs taken from the environment by using these weight and bias values. In this study forecaster is embedded into the optimization code like a function to be optimized.

3.7 Results of the Optimization

Optimization process is based on the multidirectional search algorithm which is an algorithm derivated from direct search methods for multivariable nonlinear functions [29] as explained in Chapter 3. The goal of the optimization process is to find the point, where the cost function has the minimum value without excessing the given constraints.

The optimization code searched the design space with, 0.5° sensitivity for β_2 and φ_2, 0.001 sensitivity for ζ and 0.075 sensitivity for incidence and blade tip depth. The design space that's searched for the optimization includes

approximately 1.2×10^9 samples. The optimization routine restarted for about 72 times in different start locations in order to prevent an error based on finding local minimum instead of global one. The resulting configuration obtained from the optimization study is given in Table 3.6. The optimum meridional exit angle found as 50° which shows that the minimum cost is obtained by a mixed flow impeller which is an expected result. Likewise, the values of other parameters are reasonable for an impeller design. From the structural point of view blade exit angle is reasonable for an impeller design, but it must be investigated with structural analysis tools and probably an additional structural optimization will be needed because of high loading conditions born from high rotational speed.

Table 3.6 – Resulting configuration of the optimization study

Parameters	Cost	Power (kW)	φ_2 (°)	β_2 (°)	Incidence (°)	ζ	b_2/b_1
Results	12.1158	85.9803	50	24	1.425	0.39	0.2375

3.8   Final Compressor Design

As the optimum configuration is determined, the final design is generated by using NREC according to the given configuration. Unlike the previous part of this study the final design is generated after a more detailed study by using one and two and three dimensional solvers of NREC.

It is first needed to made the design in one dimensional environment, which is the process handled with Compal. As the decision parameters selected in optimization are convenient to the inputs of Compal, it is possible to directly apply the parameters in the optimization problem to the program. According

to the optimization results, inputs of Compal are given in Table 3.7. In the last four rows of this table, the constants which determine the performance behavior of impeller according to the TEIS and Two-Zone models are given. These constants are crucial for the correctness of the performance obtained from the program. Effectiveness values, called η_a and η_b were given as 0.65 and -0.2 in the design. These values show that a poor diffusing behavior is modeled at the inducer and instead of diffusing, an accelerating characteristic is modeled at the exit of the impeller. This is a poor aerodynamic performance and it is completely consistent with the physical reality of this kind of a compressor. DR_{stall} is determining the stall behavior of the compressor, which is set as 1.4 based on the literature. M_{sec}/M is a parameter which sets the ratio of wake flow to jet flow at exit and it is given as 0.2. Likewise, this parameter is also determined from the literature.

The outputs of Compal according to the given inputs are summarized in Table 3.8. It can be seen from this table that, in case of satisfying the mass flow need, pressure ratio couldn't be conserved at the range of 5 and there is also a slight decrement in efficiency, given as 0.718. Nevertheless the power constrained is conserved at 84 kW power consumption, which is under the maximum limit of 90 kW. Although there seems to be a problem about satisfying the pressure need of 4.8, the compressor is not modified anymore in this step due to two reasons, first of all there is a pessimistic performance modeling working behind the design, so the actual performance must be a little bit higher and this is a superior performance compared with a regular radial compressor design.

Table 3.7 – Inputs of Compal

Mass flow rate	Kg/s	0.38
Rotational speed	rpm	120000
Pressure Ratio	kW	5
Rotor inlet diameter ratio (ζ)	-	0.39
Blade Height Raito (b2/b1)	-	0.2375
Incidence	Deg.	1.425
Meridional Inlet angle	Deg.	100
Blade Number	-	7
Splitter Number	-	7
Impeller type	-	Open
Tip Clearance	mm	0.2
Meridional exit angle	Deg	50
Impeller Axial Length	mm	40
Thickness @ trailing edge	mm	1.2
Backsweep angle	Deg	-24
η_a	-	0.65
η_b	-	-0.2
DR_{Stall}	-	1.4
M_{sec}/M	-	0.2

Table 3.8 – Geometry and performance characteristics at on-design point of the final design

Mass flow rate	Kg/s	0.388
Rotational speed	rpm	120000
Power	kW	84.1
Efficiency	-	0.718
Pressure Ratio	-	4.34
Inducer hub radius	mm	11.3
Inducer tip radius	mm	29
Inlet Tip Beta angle	Deg(mrd)	-58.2
Tip Relative Mach Number	-	1.2
Exit tip radius	mm	43
Blade tip depth	mm	4.2
Meridional exit angle	Deg	50
Impeller Axial Length	mm	40
Backsweep angle	Deg	-24

Performance Map, generated from Compal is shown in Figure 3.12. The pressure drop characteristics towards choke in the figure may seem to be unrealistic at first, however it should be noticed that this plot shows the performance characteristics only for the impeller instead of the entire stage. Only constraint that couldn't be conserved is operating range which is calculated as 0.15 while 0.2 was the minimum limit for the optimization problem. As the one dimensional design in Compal is finished, it is passed through the two and three dimensional design by using Axcent. Although Axcent is able to construct three dimensional geometry with the two dimensional flow analysis, it is not possible to use second feature due to the high speed flow structure in the passages of current design. So that only the generation of the three dimensional geometry is completed in Axcent and the flow analysis is made by using three dimensional flow solver in Pushbutton CFD. The three dimensional geometry generated from the AxCent is shown in Figure 3.13 with its side views. The additional geometric features like passage area, blade angle distribution and thickness distribution are also added to the results which are given in Appendix A.
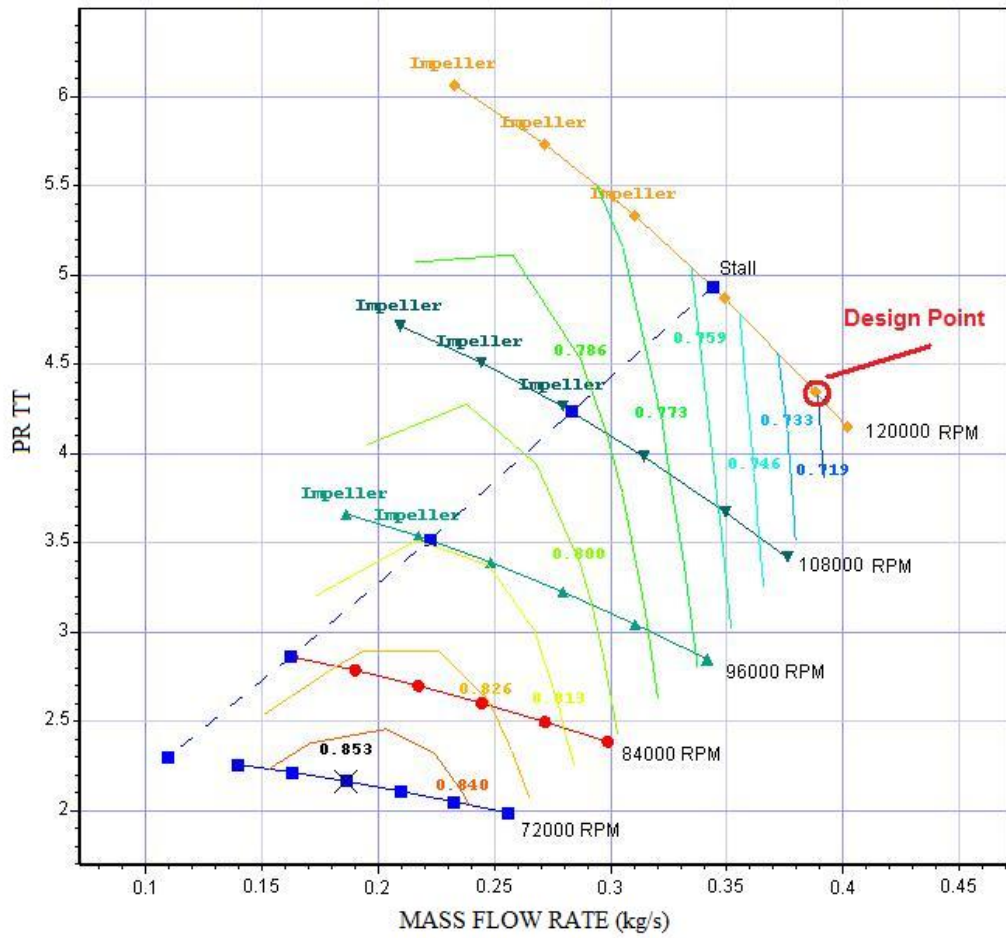
Figure 3.12 – Performance Map generated from Compal

After constructing the full geometry, CFD analysis is made by using Pushbutton CFD in order to finish the study and see more precise performance results. This part of the study is briefly explained in next Chapter.
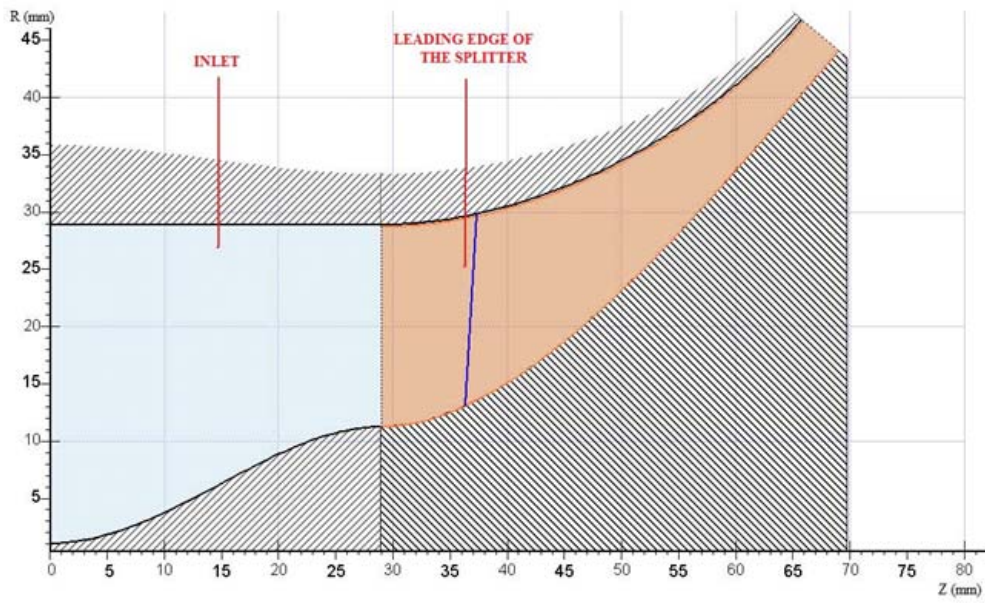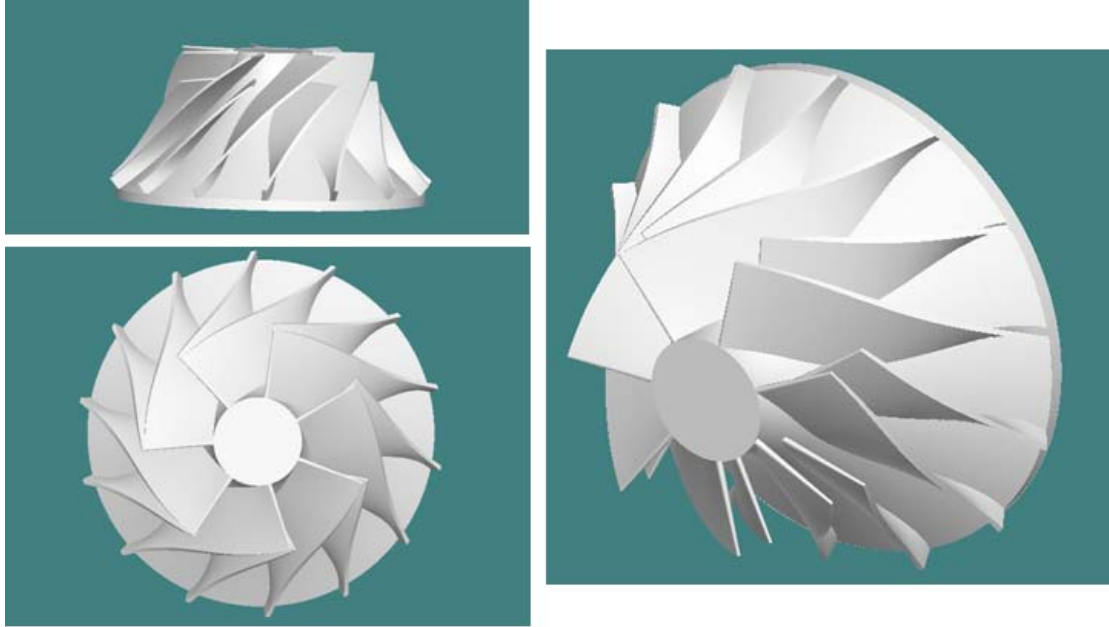
Figure 3.13 – 3D and side view of the final design

In order to demonstrate the effect of current optimized design characteristics to the engine performance, the engine cycle code is run using the design point performance data of the final design. The engine performance is found as, 240 N thrust while consuming 0.013 kg/s of JP-8 fuel at design point. These results are compared in Table 3.9 with a small jet engine which has a typical radial compressor [34]. Comparison is given in table 6, which shows that it is possible to reach a higher performance with less fuel consumption relative to a engine with purely radial compressor. The only thing to be noticed here is the, results did not validated for an entire stage. However it is possible to say that, the resulting trends are consistent with the studies of Monig [9] and TJ series engines [10]. Consequently, current results show that the turbojet engine based on the final design is superior to an engine using a typical radial compressor.

Table 3.9 – Comparison of a radial compressor based turbojet [11] performance with the final design

Parameters	A turbojet engine with a typical radial compressor	Current Design
Mass flow rate (kg/s)	0.36	0.388
Pressure ratio	3.1	4.34
Thrust (N)	216	240
TSFC (kg/sec/N)	6.203 E-05	5.375 E-05
Flight Mach Number	0.3	0.3

Weight increment of the engine is always an important concern if it is being talked of an aero gas turbine design. So that this issue should be investigated in order to show the feasibility of a mixed flow compressor which is a design that has a bad reputation because of its weight penalty. Table 3.10 presents weight comparison of the final design with a typical radial compressor that has the same dimensions. Cast Aluminium C-355-T-6 is

taken as reference material for the calculations. Although the final design has 44% increase in impeller weight, the total engine weight only increases by 2.6%. Furthermore, the Thrust-to-Weight ratio increases 8.3% in spite of the 2.6% increase in engine weight. Consequently, it's possible to say that using a mixed-flow impeller becomes advantageous in a small-size turbojet engine.

Table 3.10 – Weight comparison of the final design with a typical purely radial impeller

Impeller Type		Radial Flow Impeller	Mixed Flow Impeller (Final Design)
Backface Thickness	mm	4	4
Shaft Diameter	mm	19.5	19.5
Impeller Tip Radius	mm	43	43
Impeller Axial Length	mm	36.6	40
Impeller Weight	kg	0.19	0.27
Engine Weight	kg	3.15	3.23
Thrust	N	216	240
Thrust to Weight Ratio	N/kg	68.57	74.24
Engine Weight Increment	%	0	2.63
Impeller Length Increment	%	0	9.29
Impeller Weight Increment	%	0	44.11
T/W Increment	%	0	8.26
Thrust Increment	%	0	11.11

CHAPTER 4

FLOW ANALYSIS OF THE OPTIMIZED IMPELLER

In order to investigate the performance of the final design, one should use three dimensional CFD analysis, due to high flow speed and three dimensional flow structures. Pushbutton CFD software which is the CFD module of Concepts NREC is used for this purpose. As mentioned in Chapter 2, the Multi-block solver is used in this study, which is a hybrid multi-block structured grid full Navier-Stokes solver under Pushbutton CFD. The thing that should be noticed about the software is, not a precise solver like Fluent. It has no advanced grid generator which is capable of investigating flow field in detail. However it is capable of monitoring general behavior of the flow field correctly and gives enough information about the flow before a detailed and time consuming CFD effort.

An H type grid is used for domain discretization in this study. The size of the grid generated for the analysis is 81x113x89 which consists of more than 814000 cells. General and detailed views of the grid structure are given in Figure 4.1 and Figure 4.2.
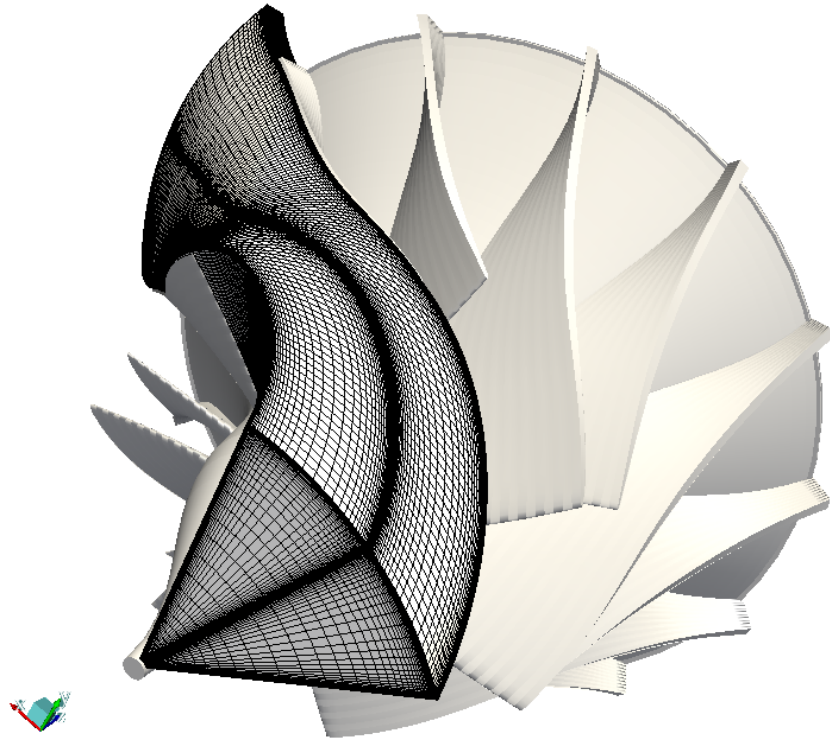
Figure 4.1 – General view of the grid
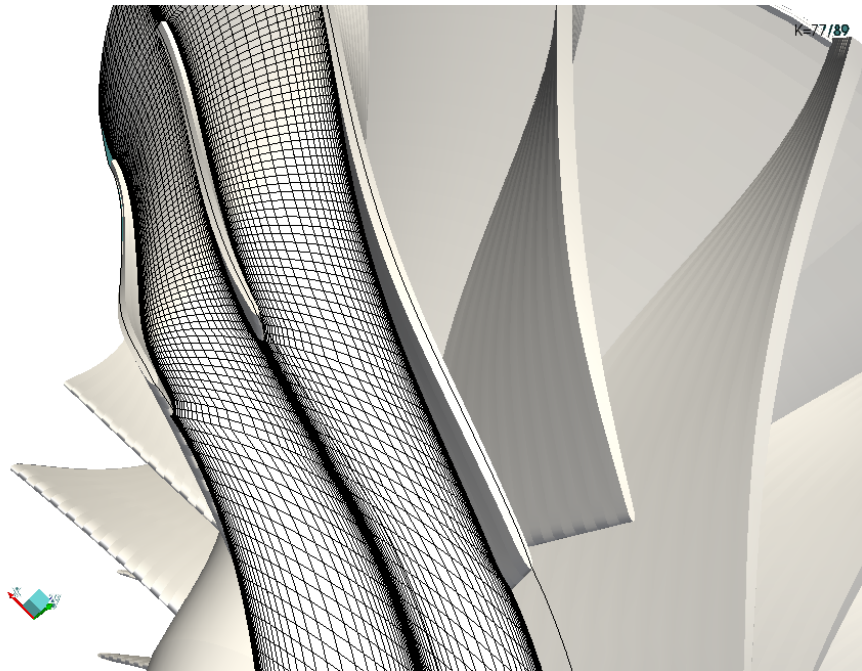
Figure 4.2 – Detailed view of the grid

Boundary conditions are directly taken from the two dimensional results of Axcent. Likewise, initialization of the grid is made by using Axcent results. Spalart-Allmaras 1-Equation model is used as the turbulence model. Log law hub/case shear stress is used as the wall treatment. Two stage Runge-Kutta method is selected as the scheme and 3rd order up-winding is selected as multi-block scheme. Analysis is made only for design conditions and each run takes about 6 hours with a Pentium Dual Core processor and 2 Gb RAM. Convergence is obtained between 1500 and 2000 iterations. First 500 iterations made with 1st order and the rest is made with 3rd order upwinding scheme.

Relative Mach Number distribution in blade-to-blade cross section from hub to shroud is shown in Figure 4.3a, b and c. In a regular compressor design with moderate rotational speed and proper aerodynamic design, the flow behavior starts with acceleration at inducer and continues with deceleration through the passage until the exit of the impeller. However, in a high speed compressor with a poor aerodynamic performance in a limited size, this phenomena turns into a continuous acceleration through the passage. Especially in Figure 4.3a, the velocity distribution near the hub section shows this kind of a flow behavior. This behavior triggers an unsurprising shock formation advancing through the shroud region which the acceleration gets more influential due to the strengthening effect of rotational speed.

In Figure 4.3b it can be seen that, there are two shock regions which occurs near the leading edge of main and splitter blades due to the mechanism explained above. Effect of weak oblique shock in the second region induces a separation at the exit of the passage. Shock wave structure gets stronger near the shroud and constitutes a shock train that continues until the separation region as shown in Figure 4.3c. Near the shroud, separation enlarges and fills most of the passage at the exit. The static pressure

distribution shows a pressure decrement near shock regions at the suction side, which continues with a smooth increment at the rest of the passage.

(a)
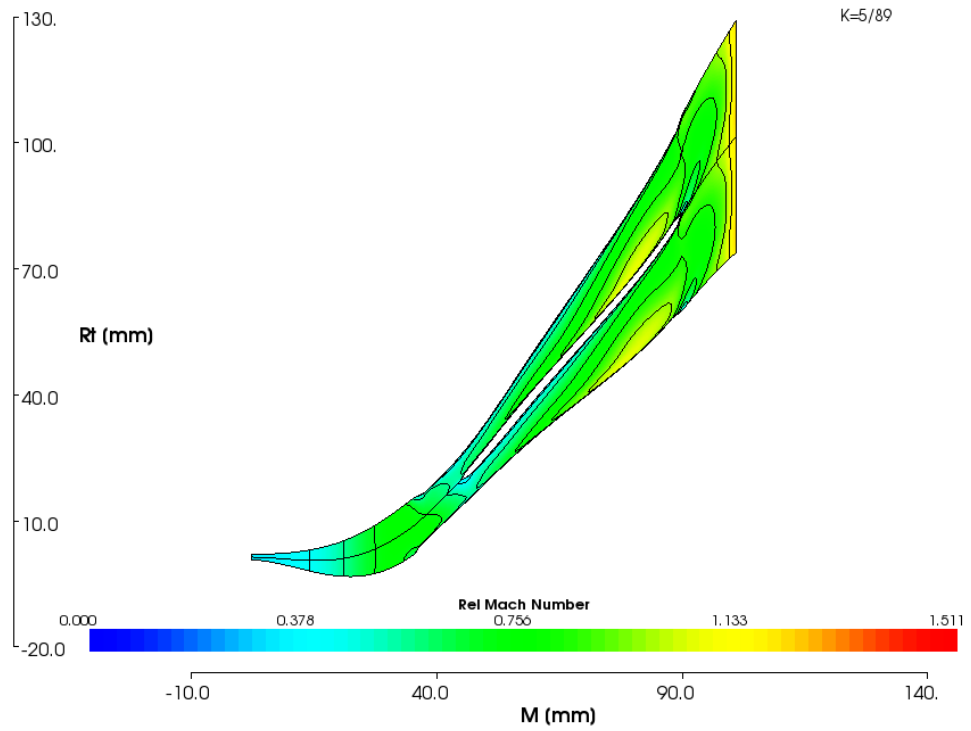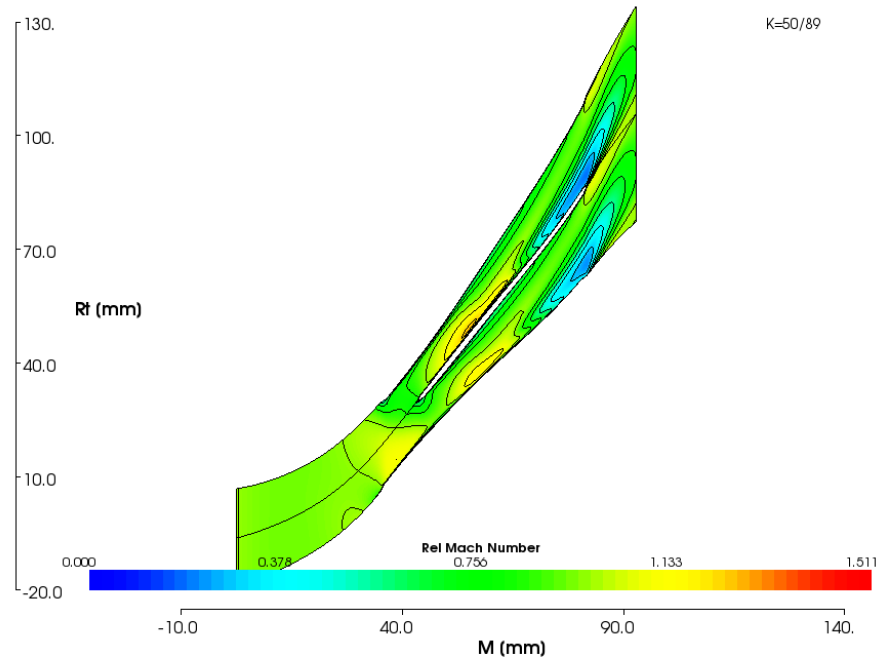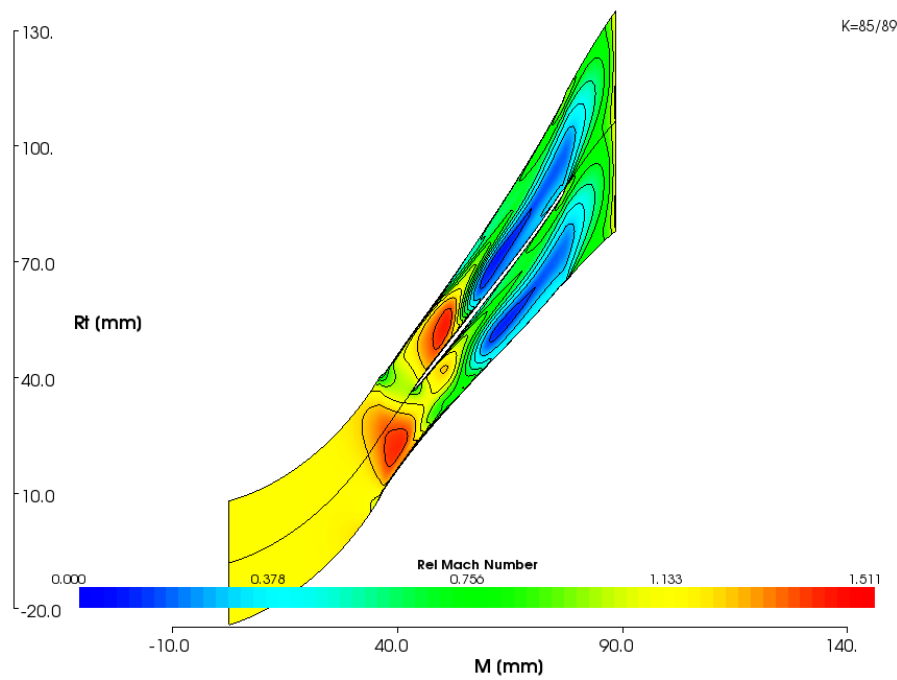
Figure 4.3 – Relative Mach Number distribution in blade-to-blade section (a) near the hub, (b) in the middle of the passage, (c) near the shorud
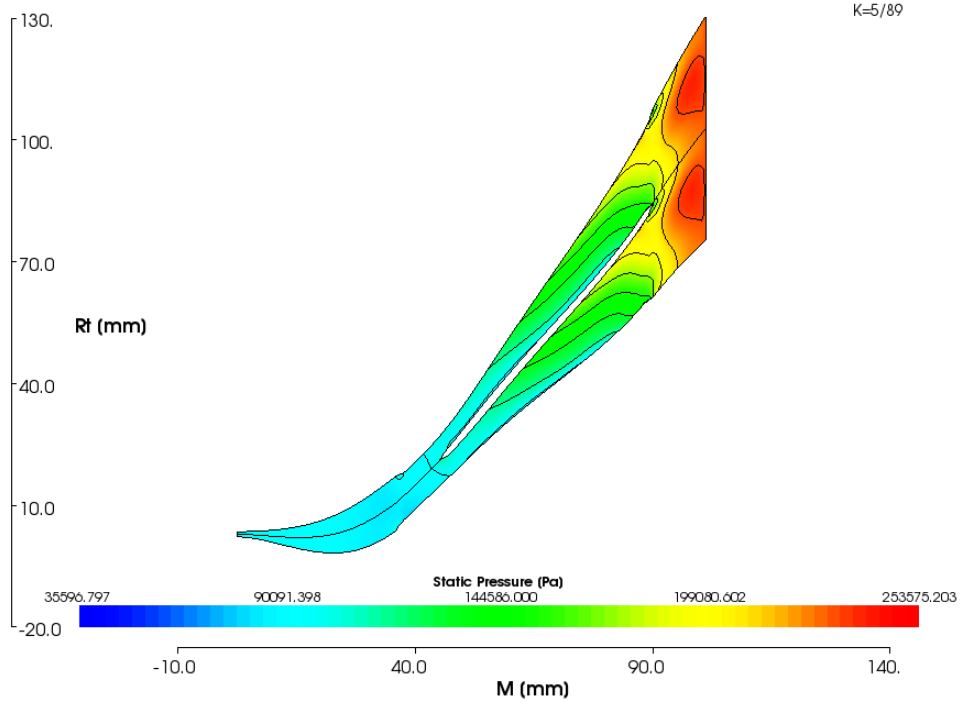
(a)
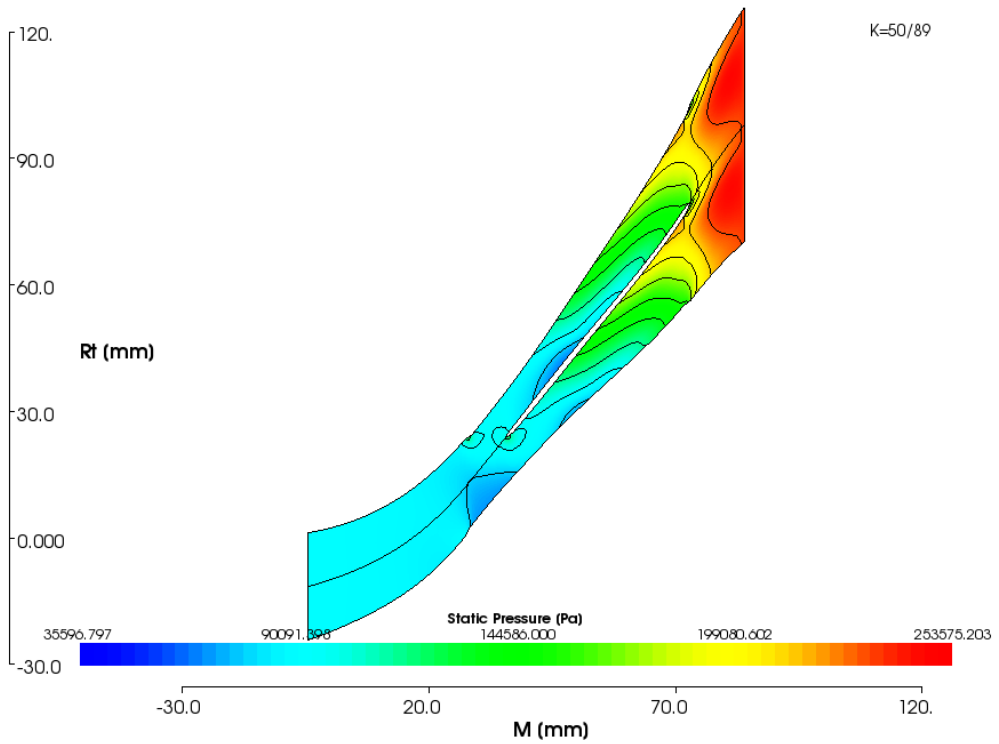
(b)
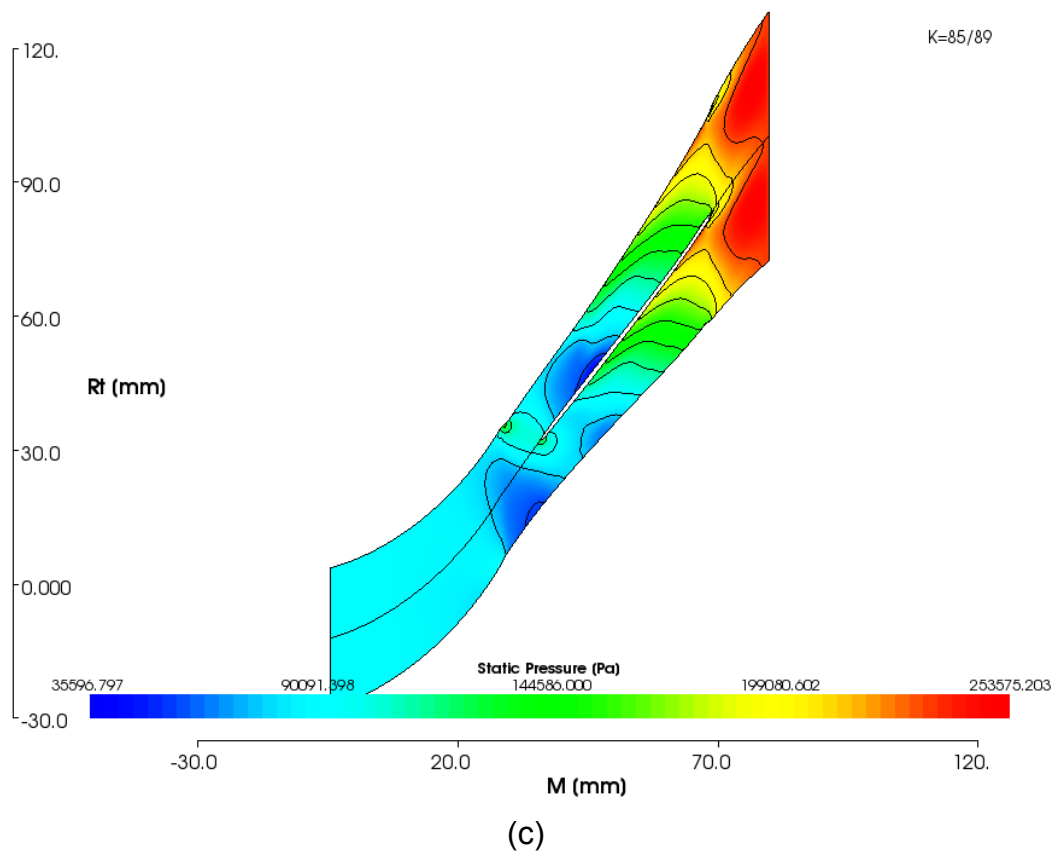
Figure 4.4 – Static Pressure distribution in blade-to-blade section (a) near the hub, (b) in the middle of the passage, (c) near the shroud

Figure 4.4 a, b and c shows the static pressure distribution from hub to the shroud in blade-to-blade plane. The shock structure that is explained on relative Mach number distribution can more obviously be seen in these figures. Especially in Figure 4.4c it can be seen that there are 3 shock waves which of two are stronger than the other on the pressure side of the passage, near the splitter leading edge.

Relative Mach number behavior of the flow from inlet to the exit can also be seen from Figure 4.5 a, b, c, d and e. The Mach Number increment with advancing through the shroud can more obviously be seen from these figures. A supersonic velocity region occurs near the shroud of suction side

and triggers an oblique shock which induces a separation region near the shroud.

(a)

(b)

(c)

(d)

84
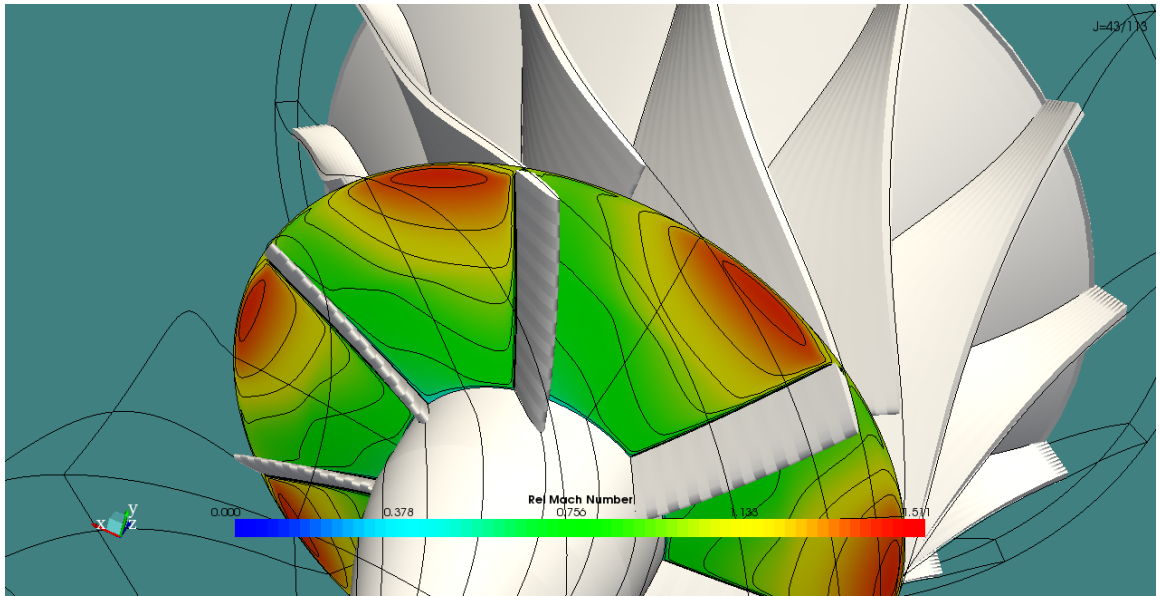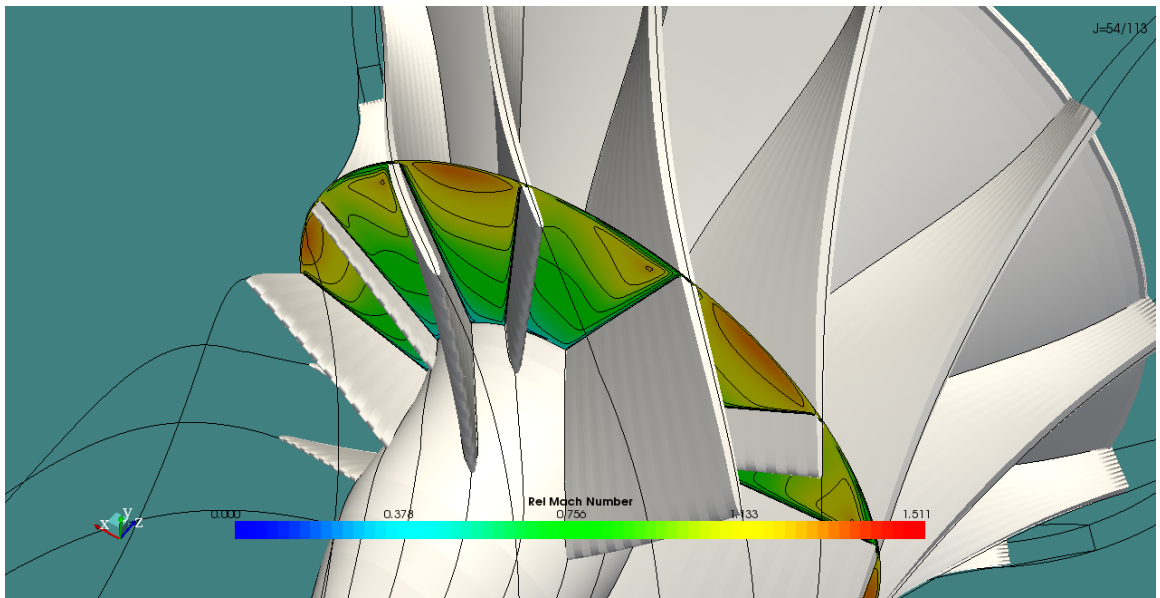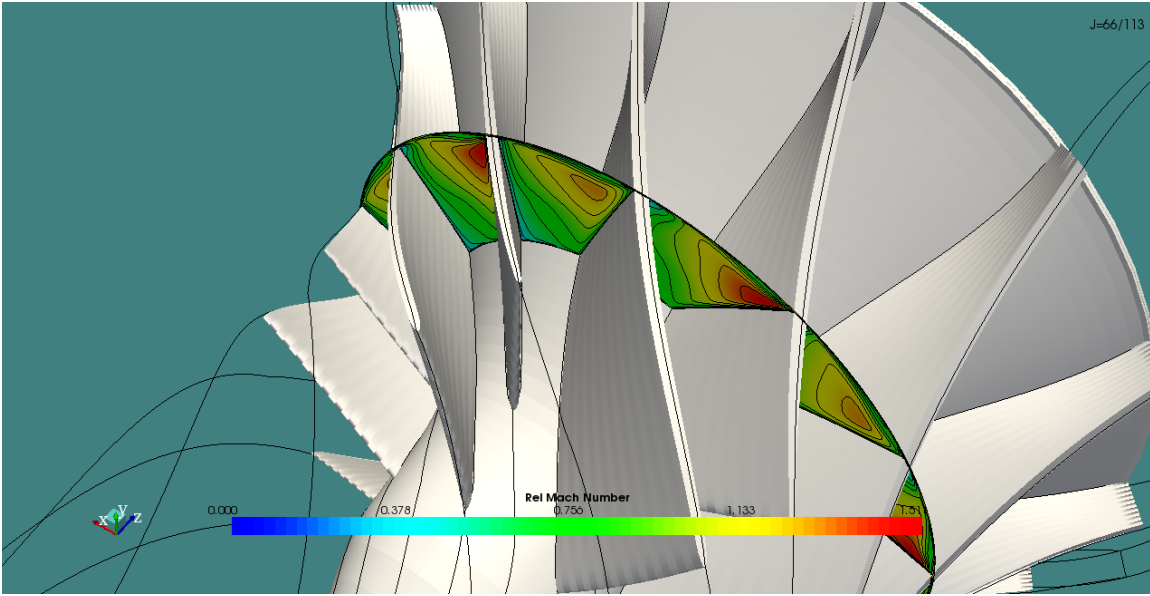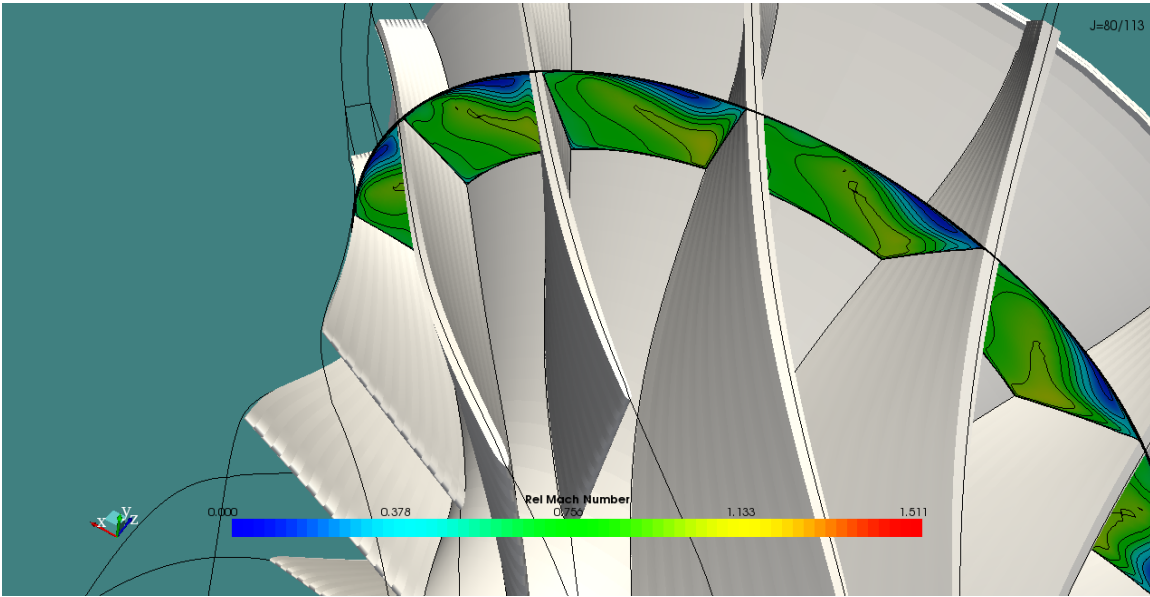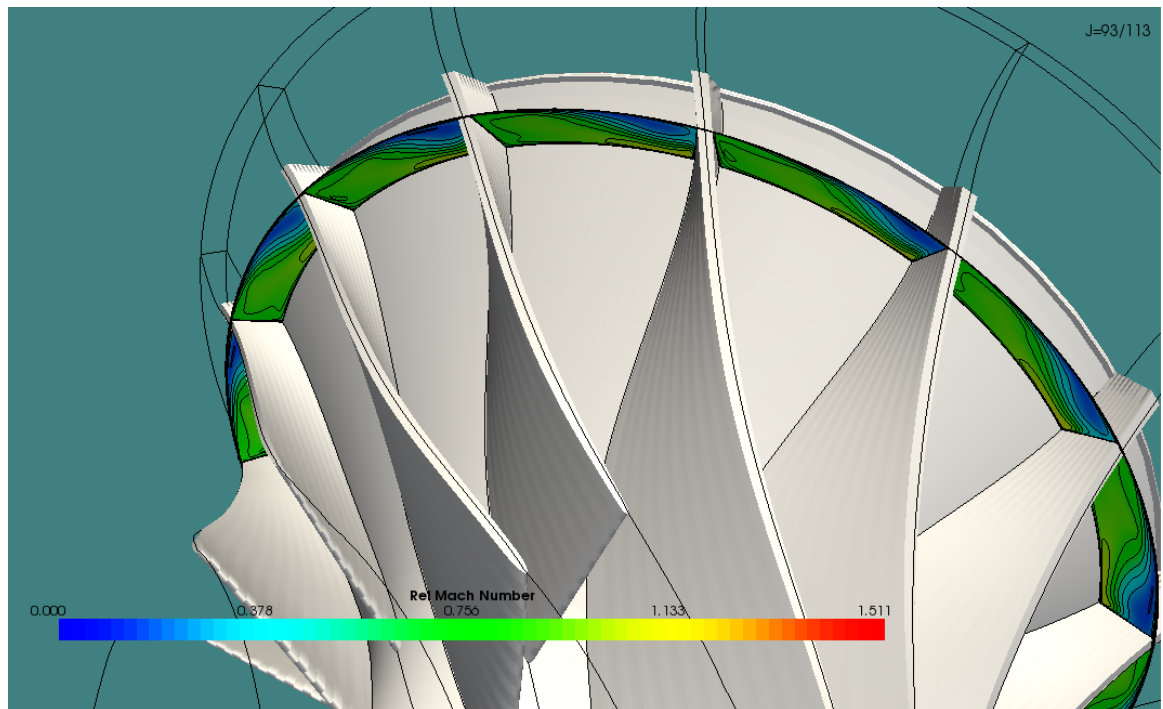
(e)

Figure 4.5 – Relative Mach Number distribution in passage section (a) near the passage entrance, (b) near the splitter leading edge, (c) in the middle of the passage, (d) in the passage where the separation starts, (e) near the exit of the passage

The results are consistent with the results of similar studies from the literature like the transonic mixed flow compressor flow analysis of Monig et al. [9] and radial flow compressor analysis of Ibaraki et al. [35]. However, detailed analysis of the final design generated from Pushbutton CFD does not give a satisfactory result from the view of aerodynamic performance. The flow pattern contains strong and continuous shock mechanism near the shroud which is followed by a wide separation region. This kind of a flow pattern is not only harmful for the design performance but also, causes numerous problems about the stability and structural life of the engine which are as important as the performance considering whole engine life. For this reason, the passage should be modified in order to improve the flow pattern.

Although using splitter is an efficient way of increasing work capacity of the rotor, the leading edge position of the splitter is a vital decision for aerodynamic behavior of the rotor entrance where high diffusion is required. According to this need it is obvious from Figure 4.3 and Figure 4.4 that, it is needed to enlarge the mass flow area to allow diffusing at the inducer. According to this need, the length of the splitter is decreased by shifting the position of the leading edge from %38 to %40 of meridional distance of the passage. The meridional cross section of the passage is enlarged in order to decrease the speed of the flow at the entrance and especially allow flow to decelerate after the oblique shock to prevent the shock train. Also the shape of the leading edge at the entrance is turned into a swept back type by giving 10 degrees meridional inlet angle, in order to weaken the oblique shock at the entrance [25]. The final form of the design is seen in figure 4.6.

Unlike the previous study, the flow investigation of the last design is made with blade-to-blade calculations due to lack of time. As it is more proper to use same type of analysis for comparison, blade-to-blade analysis of old design is used. The analysis is made with 133x331 size H type grid in %50 of the blade height and the other settings remained same with the three dimensional analysis. The results are normally not one to one coincident with the three dimensional one but they show the same results in general. So that it is possible to compare two designs by using these results.
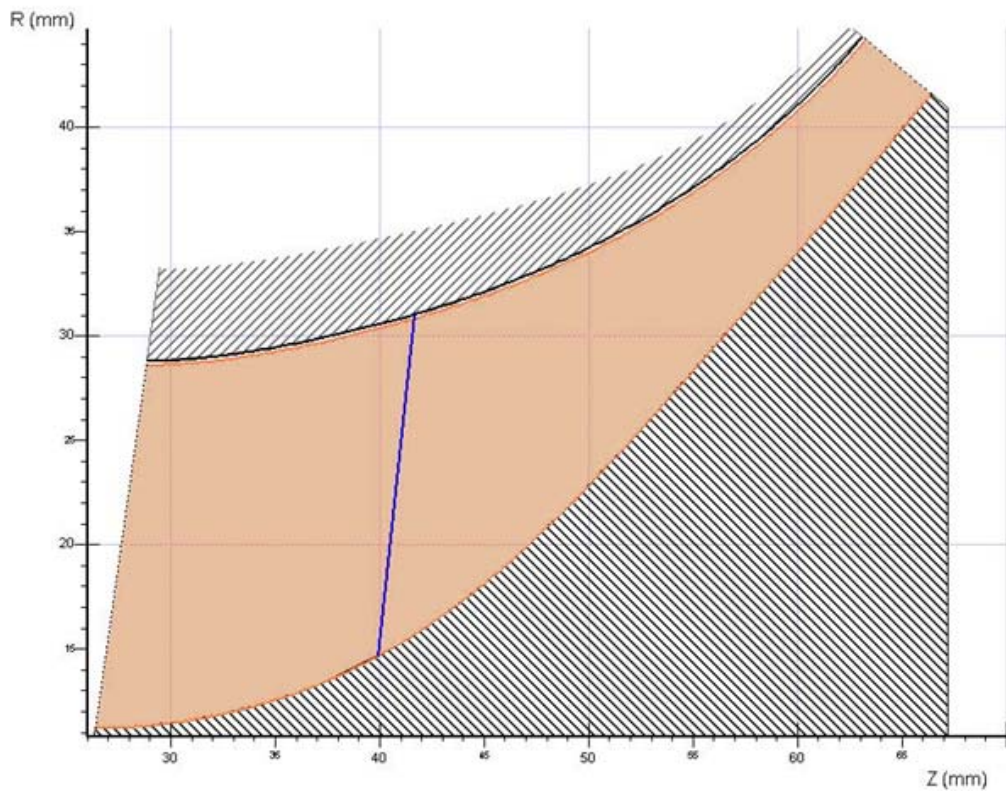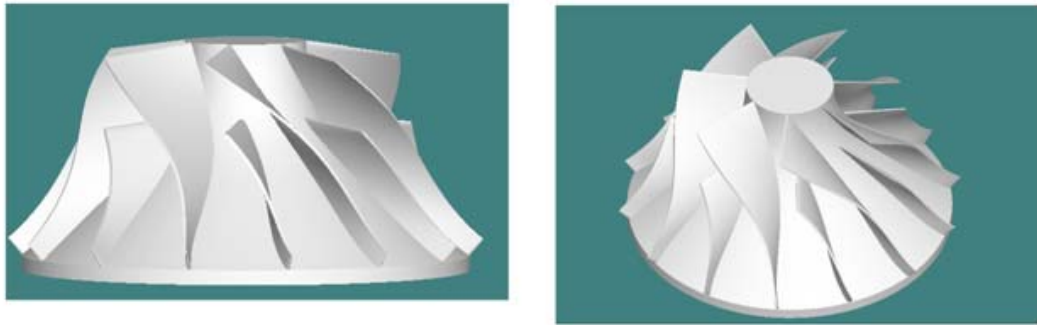
Figure 4.6 – Final form of the design after the modification

If the relative Mach number distribution is compared, the first thing that can be seen from Figure 4.7 is the disappearance of the shock train in the passage. This effect may be seen as a result of secondary flow effects in the passage, but it is possible to make this conclusion after analyzing three dimensional geometry. This also weakens the shock induced separation structure at the exit and leaves much more area to pass the flow that sustains a deceleration through the passage. Another view of this picture can be seen from Figure 4.8, which shows the static pressure distribution comparison. It can be seen that, pressure continuously and smoothly increase through the passage except the rapid increment due to the shock wave at the entrance.

The performance of the CFD analysis shows that the pressure ratio of the final design is at the range of 3.2 and 3.5. But, it should be noticed that this result is obtained from the analysis of a single rotor without including the diffuser. However, in case of adding diffuser design to this study, the performance loss will not be less dramatic due to the supersonic exit of rotor which should be regulated in a very limited area.
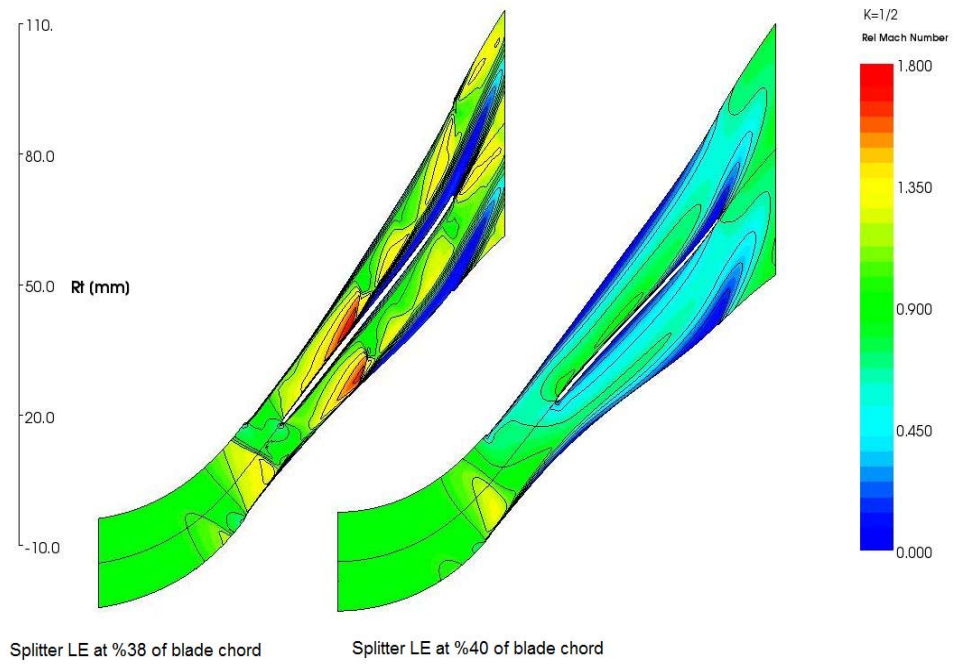
Figure 4.7 – Comparison of the relative Mach number distribution of the first and the modified design in the middle of the hub-to-shroud section
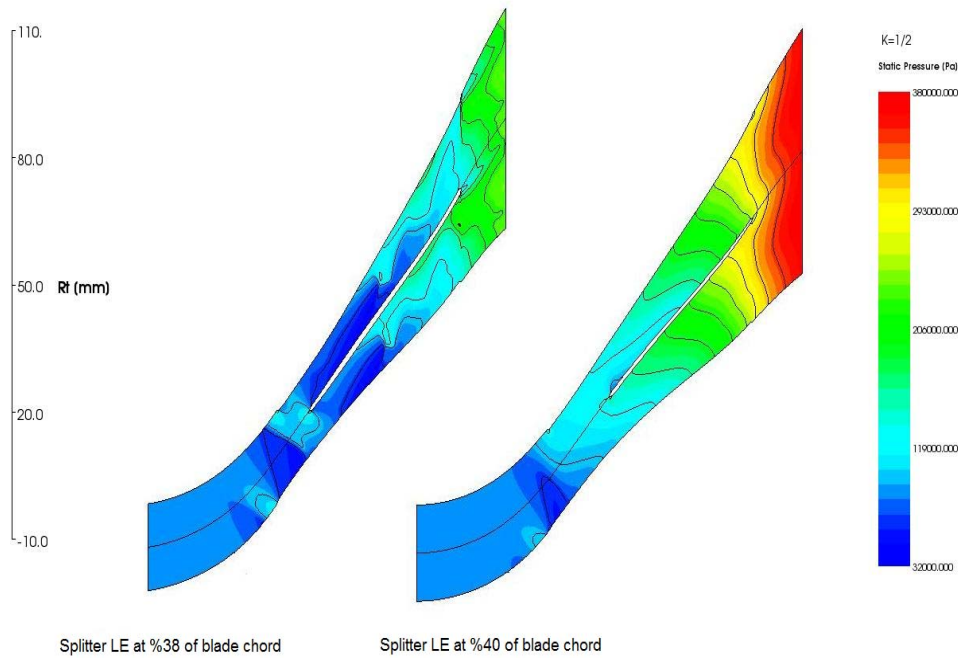
Figure 4.8 – Comparison of the static pressure distribution of the first and the modified design in the middle of the hub-to-shroud section

CHAPTER 5

CONCLUSIONS AND DISCUSSIONS

In this thesis, a design and optimization study is performed by following steps of a methodology, for obtaining an optimum configuration for the impeller of a small mixed-flow compressor that can be used in small aero gas turbine engines. The performance of the design has been investigated by CFD and the final design is shaped by making necessary modifications according to the CFD results.

The design methodology is based on generating a configurational database for various compressor geometries using 1D design codes and a turbomachinery design/analysis software, application of Design of Experiments to properly sample the design space, representing the cost function variations within the design space through a Neural Network and then finding the optimum configuration that minimizes the cost function. This procedure is applied for designing the impeller of a mixed flow compressor. The optimum values for a set of design variables that maximize a cost function based on the specific thrust and the TSFC of the engine is obtained. A sample design optimization study showed that the designed compressor as well as the engine has improved performance characteristics when compared to a typical small turbojet engine and its small radial compressor without exceeding the weight limitations.

On the last part of the study, CFD analysis of the optimized design has been made at the design point, by using the same commercial software. The

results of the analysis showed that there are shock and separation regions in the blade passage which can cause unsteadiness in operation regime and lack of performance. A second design is generated by making modifications on the first and it has been investigated again by using CFD. The modified design showed a better flow characteristic in the passage. Although the results should be compared with experimental data for validation, the results show a good consistency with the literature.

Although the parametric calculations foreseen the pressure ratio of 5, CFD results shown the realistic performance of a conventional radial compressor geometry [8]. However, as mentioned before, the target of 5 pressure ratio is not an unrealistic target that, the possibility of which has already shown by Monig et al. [9] However, these examples are based on some unconventional radial compressor concepts that may be investigated as an extension of this study. So that it is possible to say that, although the targets are not unrealistic, it is hard to achieve them by a conventional design.

Future work in order to improve this study, can focus on three different topics which are,

- Repeating the same study by using a better database based on experimental mixed flow compressor data
- Improving the CFD analysis by using a more precise CFD code and grid generator
- Improving the methodology by adding diffuser design tools and making a full stage design optimization study.

REFERENCES

[1]   UAV Roadmap 2005-30. Department of Defence, 2005 August, Appendix D

[2]   Eisenlohr G. and Benfer F. Wilhelm, Aerodynamic Design and Investigation of a Mixed Flow Compressor Stage, AGARD CP-537; 1993

[3]   Mönig R . Broichhausen K.D. and Gallus H.E, "Application of highly loaded single stage mixed-flow compressors in small jet engines," AGARD CP-421, 1987.

[4]   Goldstein A. W, "Design and test of mixed flow impellers," NACA Research Memorandum E8F04., 1948.

[5]   Douglas E.J., Schwartz R. I., 1946, "Tests of Cast Alluminium Alloy mixed Flow Impellers," NACA Memorandum Report E6C07.

[6]   Harmick J. T., Ginsburg A., Osborn W. M., "Method of analysis for compressible flow through mixed-flow centrifugal impellers of arbitrary design," NACA Technical note 2165, 1950.

[7]   Stanitz J. D., "Two Dimensional Compressible Flow in Conical Mixed Flow Compressors," NACA Technical Report No 1744, 1948.

[8]   Musgrave, D. S., and Plehn, N. J. "Mixed-Flow Compressor Stage, Design and Test Results With a Pressure Ratio of 3:1," ASME Journal of Turbomachinery, Vol. 109, pp. 513-519

[9] Mönig R. Elmendorf W. and Gallus H.E. Design and rotor performance of a 5:1 mixed flow supersonic compressor. Journal of Turbomachinery; Volume 115, July 1993

[10] Harris M.M. Jones A.C. Alexander E.J. Miniature turbojet developement at Hamilton Sundstrand the TJ-50, TJ-120 and TJ-30 turbojets. AIAA 2003-6568. 2nd AIAA Unmanned Unlimited Systems. Technologies, and Operations — Aerospace. San Diego. California; 2003

[11] Pauer R., Nrobert M., Impeller Design for Radial and Mixed Flow Compressors. IMECE2004-61926, Proceedings of IMECE 04 ASME International Mechanical Engineering; Anaheim California; November 2004

[12] Stanitz J. D., Prian V. D., A Rapid Apprximate Method for Determining Velocity Distriburion on Impeller Blades of Centrifugal Compressors, NACA Technical Note 2421; July 1951

[13] Japikse D. And Pratt M. Optimization in component design and redesign. The 10th International Symposium on Transport Phenomena and Deynamics of Rotating Machinery; March 2004

[14] Pelton Robert J., One Dimensional Radial Flow Turbomachinery Performance Modeling, M.Sc. Thesis, Brigham Young University, 2007

[15] Benini E. Optimal Navier-Stokes design of compressor impellers using evolutinary computation. International Journal of Computational Fluid Dynamics Vol.17, pp.357-369; 2003

[16] Kim J.H., Choi J. H., Kim K. Y., Design Optimization Of A Centrifugal Compressor Impeller Using Radial Basis Neural Network Method, GT2009-59666, Proceedings of ASME Turbo Expo 2009, June 8-12, 2009

[17] Mouli C. Srinivas J. and Subbaiah K.V.Optimization and output Forecasting using Taguchi-Neural Network Approach. IE Journal; Vol 86, March 2006

[18] Mattingly J. D. Heiser. W.H. Pratt D. T. Aircraft Engine Design. AIAA Education Series; 2002

[19] Hill P. G., Peterson C. R., Mechanics and thermodynamics of propulsion, Reading, Mass: Addison-Wesley, 1992

[20] Cumpsty N. A., Compressor Aerodynamics, Longman Scientific&Technical, 1989

[21] Eckardt D., Instantaneous Measurements in the Jet-Wake Discharge Flow of a Centrifugal Compressor Impeller, Journal of Engineering for Power, pp. 337-345, 1975

[22] Dean R. C., Senoo Y., Rotating Wakes in Vaneless Diffusers, Journal of Basic Engineering, 00. 563-574 1960

[23] Japikse D., Assessment of Single and Two Zone Modeling of Centrifugal Compressors, Studies in Component Performance, ASME Paper No.85-GT-73, 1985

[24] Wiesner F. J., A Review of Slip Factors for Centrifugal Impellers, Trans. ASME, Journal of Engineering for Power, pp.558-672, 1967

[25]   Japikse J. D., Baines N.C., Introduction to Turbomachinery, Concepts ETI Inc., Norwich, VT, and Oxford University Press, 1994

[26]   Japikse J. D., Centrifugal Compressor Design and Performance, Concepts ETI, Inc., Wilder, VT, USA, 1996

[27]   Taguchi, G. Konishi S. Orthogonal Arrays and Linear Graphs. American Supplier Institute; 1987

[28]   Phadke M. S., Quality Engineering Using Robust Design, Prentice-Hall International Editions; 1989 pp43 pp 277-279

[29]   KELLY C. T. Iterative Methods for Optimization in Applied Mathematics; SIAM 1999.

[30]   Lewis, M. Lewis, Torczon Virginia, Trosset Michael W., Direct Seacrh Methods: then and now, Journal of Computational and Apllied Mathematics Vol. 124, pp. 191-207, February 2000

[31]   Belegundu Ashok D. and Chandrupatla Tirpathi R., Optimization Concepts and Applications in Engineering, Prentice-Hall, 1999

[32]   Haykin Simon, Neural Networks a Comprehensive Foundation, Second edition, Prentice Hall, 1999

[33]   Mouli C. Srinivas J. and Subbaiah K.V.Optimization and output Forecasting using Taguchi-Neural Network Approach. IE Journal; Vol 86, March 2006

[34]   Lichtsinder Michael and Levy Yeshayayou Jet Engine model for Control and Real Time Simulations. Journal of Engineering for Gas Turbines and Power; Volume 128; October 2006

[35] Ibaraki S., Sumida K., Suita T., Design And Off-Design Flow Fields Of A Transonic Centrifugal Compressor Impeller, GT2009-59986, Proceedings of ASME Turbo Expo 2009, June 8-12, 2009

APPENDIX A
GEOMETRY DATA OF FINAL DESIGN
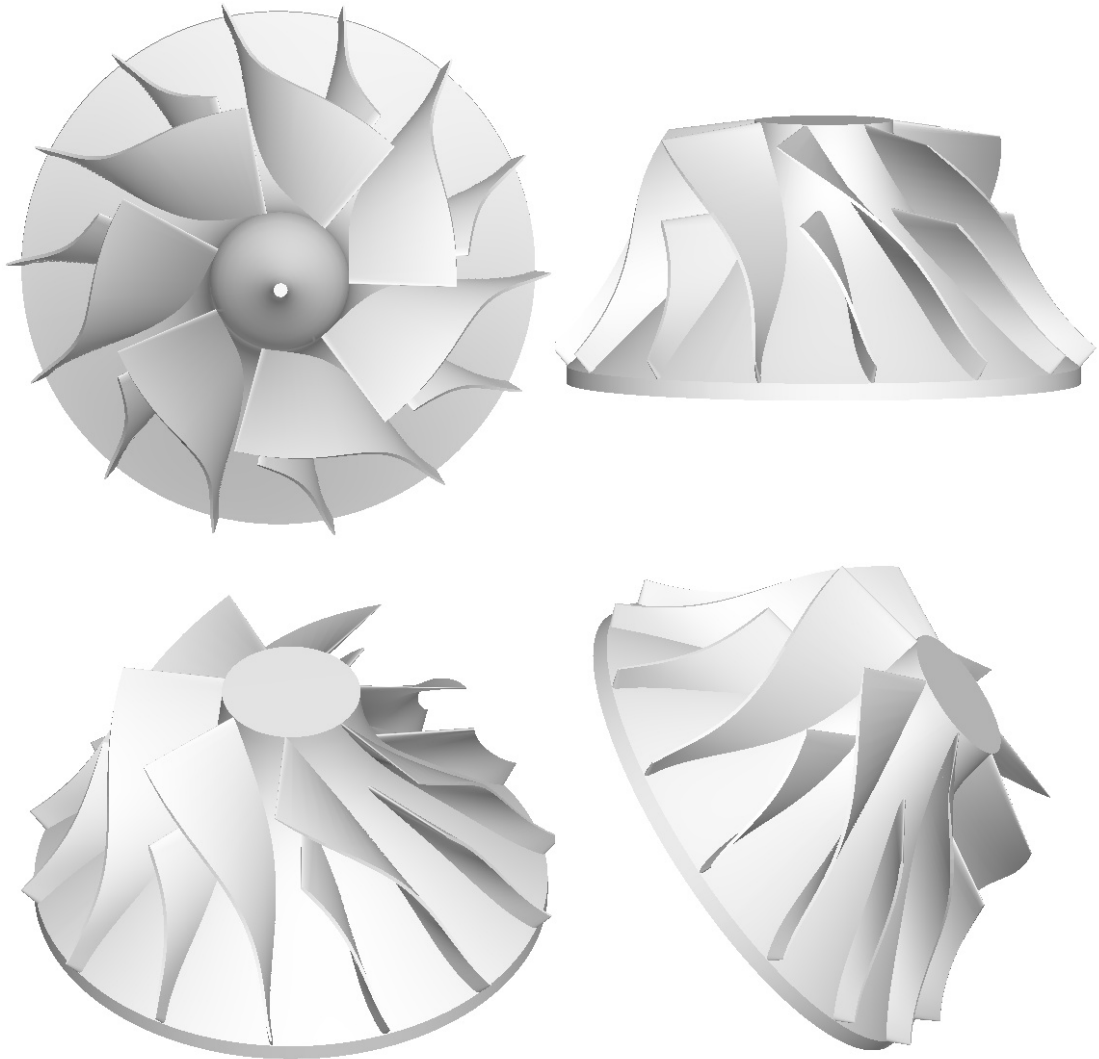
Figure A.1 –Three dimensional views of final impeller design
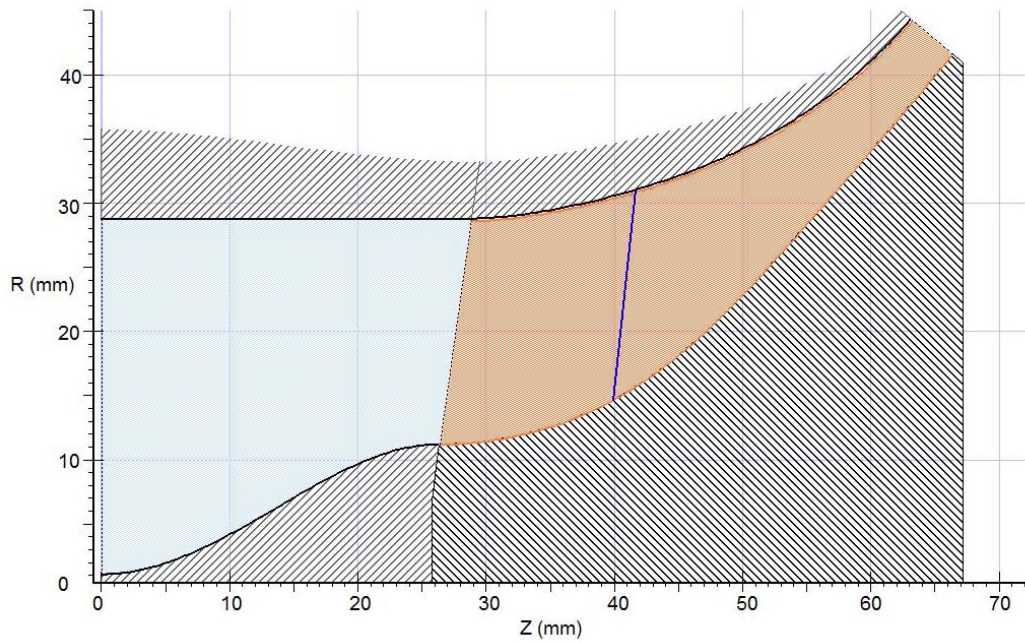
Figure A.2 – Meridional section view of the final impeller design with the inlet section
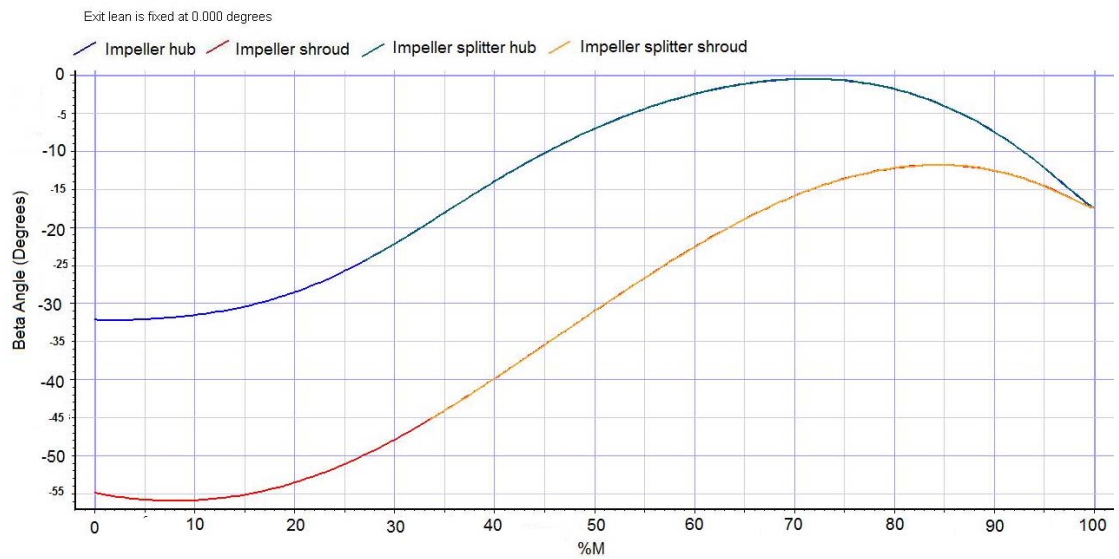
Figure A.3 – Beta Angle distribution through the passage
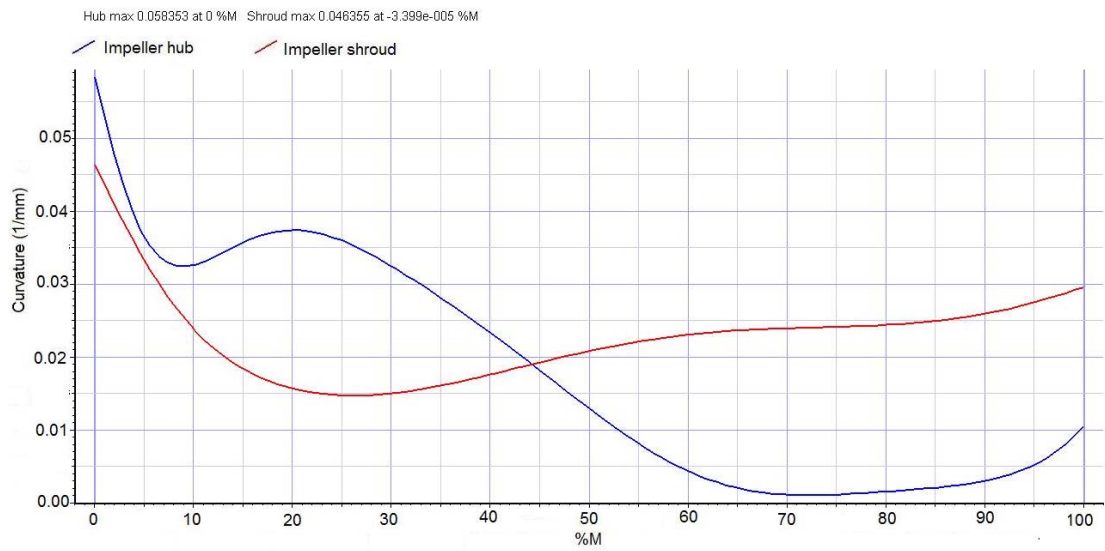
Figure A.4 – Curvature distribution through the passage
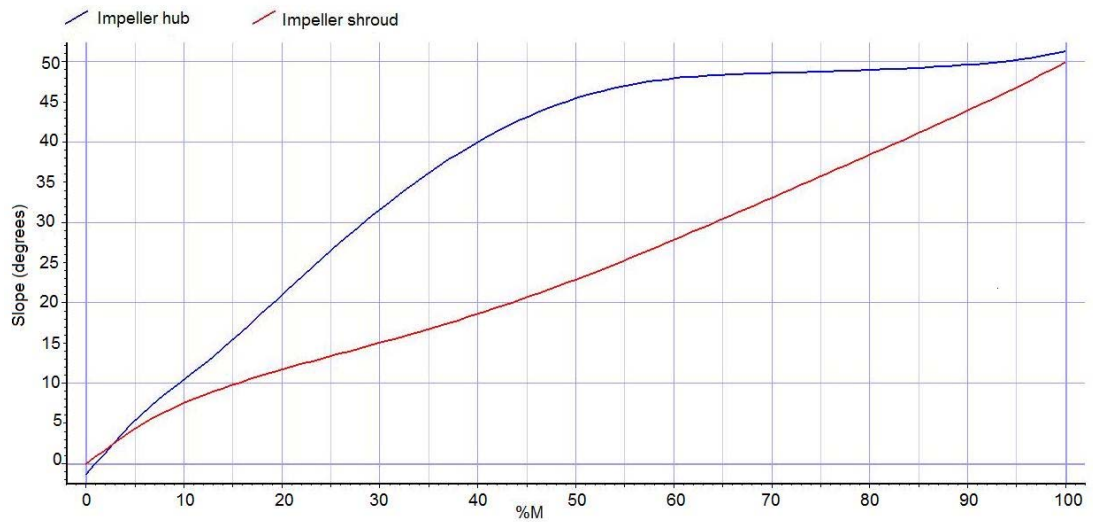
Figure A.5 –Slope distribution through the passage
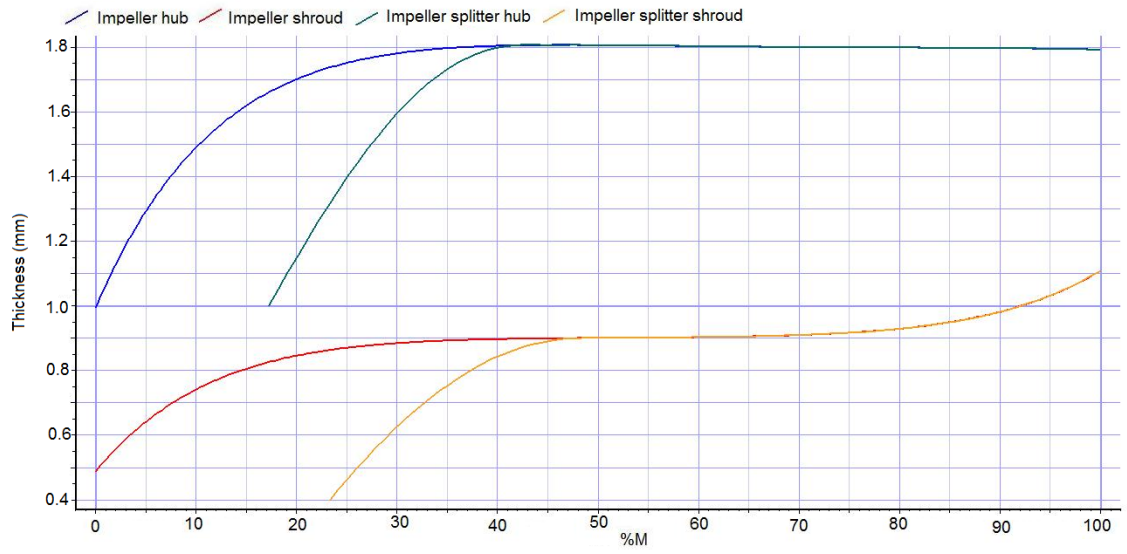
Figure A.6 – Thickness distribution through the passage